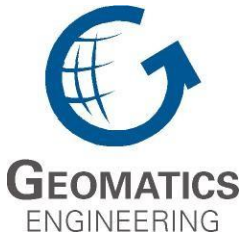

UCGE Reports
20401

Department of Geomatics Engineering

Monitoring Regional Vegetation Changes in Seward Peninsula, Alaska, Using Remote Sensing Technique

(URL: http://www.geomatics.ucalgary.ca/graduatetheses)

by

Ji Young Ahn

April 2014

Abstract

Arctic vegetation has been undergoing various transitions depending on its regional characteristics and numerous contributors to these changes include direct human impact and natural changes in the earth's climate system. The commonest causes of the vegetation change over a large arctic area are climatic. The Seward Peninsula in Alaska was reported diverse vegetation variations induced by possible climatic factors such as warming and drought conditions. Satellite observations have provided retrospective research on vegetation density patterns and changes over a long period in Arctic tundra environment. Landsat imagery has allowed documentation of spatial and temporal vegetation changes and investigation of the relationship to regional weather variations. Completed within this thesis are time-series NDVI maps of Council area in Seward Peninsula performed by both NDVI and change detection methods between 1999 and 2009. The study of vegetation change conducted here are important for monitoring the variations from the past to present and exploring the possible response to the annual weather changes.

Acknowledgements

I would like to express my heartiest gratitude to my supervisor Dr. Jeong Woo Kim for the precious insight and valuable guidance, support and suggestions throughout my master study. I tender my gratefulness and thanks to the professors, Dr. Xin Wang and Dr. Quazi K. Hassan for their advice and valuable lessons on my courses. I would like to thank Dr. Mryka Hall-Beyer for valuable lesson and knowledge on my research. This thesis could not have been completed with her considerate assistance. I would also like to acknowledge Korea Polar Research Institute (KOPRI) for providing research opportunity and support for improving my research regarding field data collection.

I would like to thank my family, my father and mother for always believing in me, for their love and unlimited supports and my life partner who always gives continues encouragement and love, and respects my decisions.

I would like to thank Jin Baek, Eunju Kwak, and Mohannad Al-durgham for sincere support in all my struggles and frustrations and valuable encouragement to make me always positive in my life here. Lastly I want to thank my supportive friends for their constant encouragement to keep me smiling always.

Dedication

I would like to dedicate this thesis to my dear parents, Mr. Taekyu Ahn and Mrs. Haeran Lee who always encouraged me not to give up in every situation and respects my decisions to start my graduate study. I am so blessed that I am a daughter of my strong and supportive parents. I also dedicate this thesis to my sister Jisung Ahn and my brother Sehoon Ahn who provide me with a strong love shield. Special dedication goes to my life partner Kunwoo Cho who gives me endless love and precious support.

Table of Contents

List of Tables

List of Figures and Illustrations

List of Abbreviations

Abbreviations	Definition
Landsat	Land Remote-Sensing Satellite
NDVI	Normalized Difference Vegetation Index
AVHRR	Advanced Very High Resolution Radiometer
TM	Thematic Mapper
ETM+	Enhanced Thematic Mapper Plus
MSS	Multispectral Scanner
OLI	Operational Land Imager
NIR	Near Infrared
SLC	Scan Line Corrector
USGS	United States Geological Survey
CVA	Change Vector Analysis
LST	Land Surface Temperature
ATLAS	Arctic Transitions in the Land-Atmosphere System
DN	Digital Number
LPGS	Level 1 Product Generation System
IARC	International Arctic Research Center
R	Red
G	Green
B	Blue

Chapter One: INTRODUCTION

1.1 Background and Problem Statement

The assessment and investigation of Arctic tundra vegetation is an important issue because it covers approximately six million square kilometers of the earth's surface (Laidler et al. 2008). Arctic vegetation communities have undergone various changes due to the direct effects of either human activities or the impact of natural sources such as fire, global warming, and dryness; and these changes have become increasingly visible in the last decades. These changes are broadly hypothesised to be the result of recent climate warming. In fact, the temperature is continually increasing, and the average surface temperature has risen 0.4 ℃ per decade in the Arctic and Sub-arctic regions of North America in the past 40 years (Elmendorf et al. 2012). As a consequence of this increased temperature, vegetation cover can be altered in a number of ways.

Vegetation production might be enhanced in response to warmer temperatures (Williams et al. 2000) and growing seasons may be longer as the depth of the snow decreases and it melts earlier in the spring (Groisman et al. 1994). As reported by Walker et al. (2003), a major concern in Arctic climate change research is that a warming trend would foster a deepening of the active layers by eliminating permafrost and releasing stored carbon to the atmosphere. This reduced permafrost could dry the tundra by releasing more water to the Arctic Ocean, and therefore change the Arctic systems considerably (Walker et al. 2003). Gamon et al. (2013) found that in addition to temperature, moisture is a key

variable determining the carbon balance of the Arctic tundra, which is specifically sensitive to the condition of moisture. These climate variables are possibly causing to degradation and conversion of vegetation types (i.e., moist to dry tundra). The Seward Peninsula of Alaska, which includes the study area, Council, had experienced important vegetation changes from tundra to boreal forest from 1985 to 1999, both of which might be particularly sensitive to disturbances and climate influences (Silapaswan et al. 2001). Climate influences also had prompted significant degradation of permafrost in the Seward Peninsula; and it was found in Alaska that increases in the ground temperature could be causing a roughly 50 % reduction of the area underlain by discontinuous permafrost (Lloyd et al. 2003). Therefore, vegetation may be changing as a result of climate changing. It is important to monitor the phenomena for quantitative understanding of the extent of recent vegetation changes.

The ability to investigate the dynamics of the Arctic ecosystem changes is uncertain due to the limited knowledge of historical vegetation dynamics at the landscape scale (Silapaswan et al. 2001). Ground-level sensors and high spatial resolution imaging systems (e.g., aerial photographs) have been used to monitor selected study sites to detect changes in vegetation; however, these methods face difficulties (e.g., expensive, insufficient long-term records, and limitation of dealing with large area coverage). A challenge to understanding the northern latitude ecosystem with respect to rapid climate change has been the lack of sustained observations of ecosystem processes (Gamon et al. 2013). Hence, there is a need for consistent, repeatable sampling of ecosystem properties and processes across the Arctic. Remote sensing is a good way to observe vegetation

repeatedly for understanding or quantifying Arctic vegetation changes in response to regional weather variation. Many authors have used satellite data that provide long-term and large-scale vegetation area information (Silapaswan et al. 2001; Walker et al. 2003; Stow et al. 2004; Laidler et al. 2008; Gamon et al. 2013). For instance, since early 1970, Landsat systems have been widely used to monitor vegetation cover and density throughout the Arctic tundra, and enable researchers to conduct the ecological studies by offering large amounts of no-cost data (Landsat Science Team 2010). Silapaswan et al. (2001) used the classification technique to detect vegetation cover changes in Seward Peninsula, Alaska using Landsat TM data, and Jia et al. (2003) used the time series of 21-year Normalized Difference Vegetation Index (NDVI) to monitor vegetation greenness in northern Alaska using the Advance Very High Resolution Radiometer (AVHRR).

In this thesis, due to short period of the study (i.e., less than 25 years), the vegetation type would probably not be expected to change over the study period (1999 – 2009) in Council, Alaska, and the changes with respect to climate variations would not be interpreted. However, the vegetation density may change within the study periods, and it can be investigated by remote sensing images that present us with an excellent surrogate for vegetation density in the NDVI. The results also can be explained with the annual weather changes and its trend instead of long-term climate changes. Therefore, this research should be able to observe how the vegetation density is changing if suitable images can be acquired at appropriate intervals and most of radiometric noise can be eliminated. Although this thesis only examines for 10 years, it provides a demonstration of the kind of work that can be done in a remote area with little alternative data available.

1.2 Research Objectives

The primary goal of this thesis is to evaluate vegetation changes in Council, Alaska from 1999 to 2009 by documenting changes in NDVI and exploring its relationship to weather data. This research aims to better quantify the spatial and temporal vegetation changes in response to changing weather conditions. The following conditions needed to be met:

- Appropriate multi-spectral and multi-temporal satellite data must be available for the study area.
- Effective methods must be established to identify vegetation density changes in the study area using satellite imagery.
- Supportive ancillary data must be available to interpret the results.

To achieve the goal of this study, multi-temporal Landsat Thematic Mapper (TM) and Enhanced Thematic Mapper (ETM+) data were used in this thesis to determine whether temporal spatial changes in vegetation can be detected in the Council area, Alaska from 1999 to 2009 during the summer season. Moreover, additional meteorological data were integrated in order to analyze the relations of vegetation changes to the annual weather variations (e.g., temperature, precipitation, and soil moisture). In this thesis, a satellite-derived NDVI was mainly used to monitor the vegetation density and changes of vegetation area. This thesis therefore provides information about the temporal changes in Arctic vegetation and the interactions between vegetation characteristics and climate variables. The results can demonstrate that the Landsat imagery can be used to track

ecosystem in response to annual weather change in the high latitude region and also provide the basis for future research at this spatial and temporal scale.

Chapter Two: REVIEW OF LITERATURE

2.1 Historic Vegetation Changes and Characteristics in Seward Peninsula

Historically, arctic ecosystems have included unpredictable natural events such as fire, and have in some areas been impacted by human interventions such as resource extraction. Global climate change currently threatens to have a much more widespread impact, but the details are not yet well understood because of the lack of time series of relevant data. Investigated by many researchers, Arctic landscapes are mainly characterized by vegetated area with a variety of vegetation species, and non-vegetated areas that include lakes and ponds, barren, and glacier. The unique vegetation types generally identified in Arctic tundra are spruce trees, shrub, and tundra (Raynolds et al. 2008). Much of the landscape on the Seward Peninsula in Alaska is characterized by the transition zone between boreal forest and tundra, and this transition has thought to be in flux with warming conditions by several researchers (Silapaswan et al. 2001; Raynolds et al. 2008; Gamon et al. 2013). For example, changes in shrub had occurred in this area, probably including increases in shrubbniness from 1986 to 1999, and Silapaswan et al. (2001) also found that canopy density and leaf area might increase in non-tree species. In addition, this area is underlain by discontinuous permafrost, whereas it was predominantly underlain by continuous permafrost in the past. The discontinuous permafrost appears that in the recent past due to thawing process (Stow et al. 2004; Raynolds et al. 2008). These alterations are hypothesized to be caused by increased temperatures and drying trend since 1950. Furthermore, Yoshikawa and Hinzman (2001)

conducted an investigation of the hydrologic aspects in Council, Seward Peninsula. They examined the several ponds located in the Council area and found that degradation of the permafrost beneath resulted in drainage within the ponds. Degradation in the permafrost depths due to the climate variations in Arctic regions could lead to changes in the competitive advantage of different species, and thereby result in modifying its ecosystem composition and vegetation cover characteristics (Serreze et al. 2000; Stow et al. 2004).

2.2 Background to the Landsat Program

As an Earth resource technology satellite, the Landsat program has provided the longest continuous global record of the Earth's surface since the early 1970s. Due to the continuously and consistently available data, scientists can document and assess the changes in Earth's landscape (Landsat Science Team 2010). Seven Landsat satellites have been launched successfully, namely Landsat-1 to -5 and Landsat 7-8, including recently launched mission (Landsat Science Team 2010). Through these missions, assessment of changes in vegetation properties has been investigated with the high-quality, multi-spectral, and moderate-spatial resolution image (Hope et al. 2005; Beck et al. 2005). Table 2.1 demonstrates the characteristics of the Landsat missions, and it is noted that four different sensors have been included on these missions: the Multispectral Scanner (MSS), the Thematic Mapper (TM), the Enhance Thematic Mapper Plus (ETM+), and the Operational Land Imager (OLI).

Table 2.1 : Characteristics of Landsat-1 to -8 Missions

(Lillesand et al. 2007; Landsat Science Team 2010; USGS)

Satellite	Launched	Decommissioned	Sensors	Resolution (m)	Revisit interval
Landsat-1	Jul 23, 1972	Jan 6, 1978	MSS	79	18 days
Landsat-2	Jan 22, 1975	Feb 25, 1982	MSS	79	18 days
Landsat-3	Mar 5, 1978	Mar 31, 1983	MSS	79	18 days
Landsat-4	Jul 16, 1982[a]	Jun 15, 2001	MSS TM	79 (MSS) 30 (TM)	18 days
Landsat-5	Mar 1, 1984[b]	—	MSS TM	79 (MSS) 30 (TM)	16 days
Landsat-7	Apr 15, 1999[c]	—	ETM+	30 15 (pan[d])	16 days
Landsat-8	Feb 11, 2013	—	OLI	30 15 (pan)	16 days

[a]TM data transmission failed in August 1993.
[b]MSS powered off in August 1995; solar array drive problems began in November 2005.
[c]Scan Line Corrector (SLC) malfunctioned on May 31, 2003.
[d]pan : panchromatic image.

The MSS onboard Landsat-4 and -5 contains four spectral bands (e.g., green, red, and two near infrared bands) with a spatial resolution of 79 m, and this sensor was firstly used for Arctic vegetation assessments by researchers (Landsat Science Team 2010). Subsequently, the TM was developed and is a highly advanced sensor integrating a number of spectral, radiometric, and geometric design improvements compared with the MSS (Lillesand et al. 2007). As TM products provided a higher spatial resolution of 30 m and narrower wavelengths of blue, green, red, and the near infrared regions (three NIR bands) than MSS, TM enabled researchers to provide better results for vegetation discrimination (Lillesand et al. 2007). The development of ETM+ provides more clear detailed features in the land surface with the 15-m-resolution panchromatic band. However, on May 31, 2003, image acquisition through the ETM+ was greatly influenced

by the failure of the scan line corrector (SLC), and this led to image degradation approximately covering 20 to 25 %, within the scene (Landsat Science Team 2010). Several approaches to recover the image have been developed such as interpolation from neighboring scan lines and utilization of pixel values extracted from one or more alternative acquisition dates (Lillesand et al. 2007) and successfully improved by various methods provided from the United States Geological Survey (USGS). Furthermore, Landsat 8 started providing the enhanced digital data since March 2013. It consists of more spectral bands (more of visible, near infrared, short-wave infrared, and thermal infrared bands) than previous Landsat missions, and going forward from 2013 it can continually provide higher-quality dataset to researchers for investigation of detailed vegetation features in Earth's land surface (USGS).

For this research, the use of Landsat program has strong benefits for documenting changes in terms of vegetation density as it provides long-term data covering the study area at free of cost from the USGS. TM and ETM+ with the 30m spatial resolution have been used extensively to prepare image maps. Such maps have proven to be valuable tools for ecological resource assessment in that they describe the landscape in actual detail instead of the line-and-symbol format of conventional maps (Lillesand et al. 2007).

2.3 Vegetation Characteristics and Assessment Using Remote Sensing Techniques

The Arctic ecosystem dynamics are highly influenced by the vegetation structure, and this structure reacts in different ways when recorded at satellite sensors. The pigment in plant leaves, chlorophyll, strongly absorbs visible wavelengths in the blue and red regions, and, on the other hand, the cell walls in leaves strongly reflect near-infrared wavelengths. This combination of visible and near-infrared reflectance makes vegetation distinguishable from non-vegetation features and allows some quantitative measurement of leaf density under many circumstances (Laidler et al. 2008). As remote sensing has the capability to discriminate vegetation features by way of the visible and infrared spectrum from satellite sensors, there have been several efforts to identify vegetation communities using remote sensing algorithms. One of the prominent indices is the NDVI that combines intensity information from the wavelengths of visible and near-infrared light and quantifies the concentrations of green leaf vegetation (Stow et al. 2004). Using the NDVI, change may be detected and mapped. There are several considerations in using these techniques, detailed below.

2.3.1 Application of satellite-derived NDVI

The NDVI was introduced by Tucker (1979) and Deering (1989) and can be calculated from the satellite data. It is defined as the difference between the reflectance values of the near-infrared (NIR) and red spectral (RED) regions divided by the sum of those reflectance values as follows:

$$NDVI = \frac{NIR - RED}{NIR + RED}$$

The principle behind NDVI is that chlorophyll absorbs considerable amount of incident red light, while the spongy mesophyll leaf structure reflects the near-infrared region of the spectrum (Tucker 1979; Giri et al. 2007; Hasegawa et al. 2010). Hence, growing healthy vegetation possess higher NDVI values than less greening features because of the low red-light reflectance and high near-infrared reflectance. This simple nonlinear function yields the outcomes that vary between -1 and 1, and mostly the positive values correspond to vegetation areas while the negative values represent bare soil and rock, snow, and clouds (Hasegawa et al. 2010). Therefore, many researchers have used NDVI to detect vegetation changes.

Laidler et al. (2008) examined the NDVI with relation to the percent of vegetation cover in the Arctic tundra environment in which changes of soil moisture, exposed soil, and gravel till could considerably affect the variations of vegetation communities. Derived from surface spectro-radiometer, IKONOS and Landsat 7 ETM+ data, the results showed that vegetation cover changes were highly correlated with the changes in NDVI. Exploiting NDVI was beneficial for the strong potential of modeling the vegetation growth in terms of vegetation cover over the regions. Walker et al. (2012) also studied the vegetation and its greenness in North America and the Eurasian Arctic area using both ground field information and the AVHRR data over the period (1982 – 2008). The authors employed AVHRR-derived NDVI, which provided the important facts regarding

the greening trend over that large area, and they established the results with the statistics of climate changes that the warming promoted the greening trend in tundra environments.

For arctic vegetation, NDVI was found to provide the strongest grouping capability on vegetation communities. Laidler et al. (2008) and Chen et al. (2009) used the NDVI to distinguish high productive vegetation regions within the Canadian High Arctic area. The NDVI value could provide the information on a level of photosynthetic activity among different vegetation types. Besides, the comparison of one NDVI image of a period to an NDVI image of another period can be utilized to examine vegetation-cover changes (Cakir et al. 2006). Maxwell and Sylvester (2012) applied Landsat NDVI data to visualize and analyze cropland dynamics from 1984 to 2010. They produced time-series NDVI maps from Landsat imagery and compared them by grouping the NDVI values using the density slicing algorithm. Suggested method enabled the discrimination of ever-cropped land from never-cropped land and the indication for analysis of changes in land use conversion. Therefore, the application of NDVI comparisons could provide us a useful understanding of vegetation changes.

2.3.2 Change detection techniques

Change detection is the process of identifying the differences in either land cover features or phenomena by observing them at different times (Singh 1989). As the Landsat data provides the temporal record acquired over approximately four decades, trace-back studies for analyzing change of the vegetation dynamics have been successfully

investigated. For the studies of monitoring vegetation shifts, diverse change detection techniques have been introduced such as algebra, transformation, and classification. These will be explored further below. Therefore, the suitable technique for this study area needs to be chosen from among the many possibilities.

Many of the NDVI maps discussed above have been integrated into change-detection studies. Of the various techniques, the algebra methods including image band differencing, image regression, image rationing, vegetation index differencing, and change vector analysis (CVA) are utilized widely in remote sensing (Berberoglu and Akin 2009). The greatest strengths of these methods are that they are simple, straightforward, and easy to interpret (Lu et al. 2004). They have a common characteristic as they require the process of selecting a threshold to define the changed areas (Berberoglu and Akin 2009).

Image band differencing is a common change detection approach for forested and agricultural areas and generates a residual image that demonstrates the change resulting from subtraction of images taken in different dates (Singh 1989; Berberoglu and Akin 2009). Lu et al. (2004) summarized and reviewed various change detection techniques in terms of different applications. According to their study, image band differencing is the most frequently used method for change detection in practice among the algebra-based change detection categories, particularly for the vegetation change and non-change information using multi-temporal NDVI data. Macleod and Congalton (1998) examined image band differencing for identifying the change in eelgrass meadows using Landsat

TM data from 1900 to 1992, and suggested that this technique was performed successfully to detect change and non-change areas. They utilized four bands (blue, green, red, and near infrared) and subtracted each band from one period to another, resulting in change detection maps. They found that the selection of appropriate threshold was essential for dividing a level of changes between two data. It should be noted that threshold level be determined in terms of how the NDVI changes would be occurring. Given that determining the threshold values, image band differencing technique can be highly useful when recognizing the difference levels with an application of multi-temporal Landsat NDVI data.

2.4 Relationship between Satellite-derived Vegetation Assessment and Climate Variability

Changes in Arctic vegetation are highly related to climate variability. As aforementioned, this study has the constraint of interpreting the climate variables. Generally, the climate study is based on the period more than 25 years whereas this study considers only 10 years for the climate variation analysis. Nevertheless, it would be expected from previous researches, detailed below, that vegetation density change may occur with relation to annual and/or monthly weather variations as well as the result by ten-year local climate varying trends.

At the global arctic scale, Raynolds et al. (2008) explored the relationship between the AVHRR-derived land surface temperatures (LST) and NDVI which has a spatial

resolution of 1 km. According to the regression analysis, they found that the NDVI had a positive relationship with LST based on the time-series outcomes over 22 years for a whole arctic as a 5 ℃ increase in LST resulted in increasing NDVI of nearly 0.07. Particularly, the growth in vegetated and graminoid vegetation types showed positive relation to warmer temperature while the negative relationship between NDVI and LST had found in deglaciated areas, areas with many water bodies, and high mountains. Their result explained that increase in satellite-derived temperature was likely to lead to increase in vegetation growth (NDVI) in Arctic area and established which areas might be the most vulnerable to changes in vegetation due to climate variations. In this manner, vegetation changes in northern Eurasia were analyzed by Dye and Tucker (2003) using the AVHRR data from 1982 to 1999. Their research also demonstrated that generally greening trend dominating during spring and the early part of the active growing seasons arose from the direct effects of declining snow-cover and warmer air temperatures.

For the relatively small scale, Baird et al. (2012) applied Landsat-derived NDVI to examine the vegetation growth in interior Alaska between 1986 and 2009. They found that relatively higher NDVI was found in upland vegetation areas than vegetated lowland and water areas, and the declining trend of NDVI found in the study was closely related to warm temperatures and low precipitation over 22 years. They concluded that the regional weather variation possibly resulted in limitation of growth in vegetation especially forested areas (upland). Raynolds et al. (2013) also investigated the change patterns within a tundra area in northern part of Alaska between 1985 and 2007. A total six of Landsat images were used for time-series NDVI maps, and mean NDVI had

increased at a rate of 3.2 % increase over the 22 years. Especially tussock tundra areas increased the NDVI with the higher rate than non-tussock tundra areas. However, some of high-elevation areas showed the decreasing trend in NDVI. The increases and decreases of vegetation growth could be identified depending on the land surface characteristics. According to their results, overall increases in NDVI might be highly influenced by changes in hydrology and nutrient availability, possibly as a result of thawing permafrost caused by recorded warmer temperatures and various moisture conditions.

Changes in vegetation growth in the Arctic can vary depending on the characteristics of study sites and the complex local environmental factors. For the assessment of vegetation changes, it is important to examine the study site for different possibilities of changes, and also integration of metrological data is required for detailed interpretation of changes within the study periods.

2.5 Summary

Changes in the density and species composition of vegetation have been observed by many authors in Arctic tundra regions including the Seward Peninsula, Alaska using both in-situ data and remote sensing data. In order to determine the vegetation change, ground-based data is required to be compared to historical remote sensing data. However, due to the lack of ground field data in the study area, incorporating other information is out of

the scope of this thesis. Thus, only spectral information can be utilized for monitoring and assessing the vegetation changes.

The Remote Sensing technology has proven ideal for vegetation monitoring and assessments because of its spatial resolution and spectral scope. Landsat sensors have provided the longest periods of available data and moderate spatial-resolution, detailed vegetation features can be identified in a Landsat image. Moderate spatial-resolution images for vegetation study are highly useful because it can detect and characterize human-scale variation such as vegetation growth. Moreover, the Landsat-based NDVI has been greatly applied to Arctic tundra environment, and this simple and straightforward NDVI method enables researchers to not only discriminate vegetated areas in the Arctic but also to examine the changes in vegetation density. Combining satellite-derived NDVI with change detection technique provides comparisons over time that can produce important insights. Although the process leading to changes in vegetation are complicated, analyzing remote sensing estimates of these changes over time will allow further investigation into the factors contributing to these changes (climate variability), and can thereby provide understanding of changes in Arctic ecosystem dynamics.

Chapter Three: DESCRIPTION OF THE STUDY AREA

3.1 Location and Description of the Study Area

The study area selected for this research is located in the Council area, which is approximately located 120 km northeast of the city of Nome on the Seward Peninsula of Alaska. This area, covering a 620 km^2 portion of the southern region of the Seward Peninsula, is a small community that has about 25 old buildings and several mine buildings left now. Mainly the Nome-Council road can assess to Council from Nome during the summer and it is closed on winter season. Since there did not exist weather stations, historical and statistical weather data were not available in the area of Council. As stated by Nome weather data, the average temperature of July (the warmest month) is 11.2℃ and the total precipitation of July and August are 53.6 mm and 81.8 mm, respectively (Raynolds et al. 2008).

The center of the study area (Figure 3.1) is 64°51´N and 163°41´W. The Council area is characterized by the diversity of major high-latitude vegetation types, and the vegetation transition had occurred in this area between tussock tundra and spruce forest (Beringer et al. 2005). According to previous research by Beringer et al. (2005), Council area could provide a useful indication for assessment of various high-latitude ecosystem types because various vegetation types were located in close vicinity under the same climate environment. Moreover, relatively wetter and warmer climate condition can be found in this Peninsula due to the proximity to sea coast than other northern part of Alaska.

The Council site represented tundra, low and tall shrub, and white spruce forest vegetation types. As shown in Figure 3.1, spruce forests are mainly found on the east-facing sides of hills and some of them are sporadically distributed on long the rivers and valley and southern part of the study area. The low-relief region supports open tundra and low shrub. Several small lakes, ponds, and wetlands can be seen in the low-relief region, and the wetlands mostly contains moist tundra lined with low and tall shrub and spruce trees (Beringer et al. 2005).

Figure 3.1 : Landsat TM image (left) shows the study area in the Council area, Seward Peninsula, AK, taken on 09/20/2010 with the band composite of TM3, TM2, and TM1 (R,G,B) and map of Alaska showing the Seward Peninsula (right) and detail location of Council (middle) from Google Earth.

3.2 Vegetation Characteristics

As this area is constrained by limited field data, it is difficult to achieve the detailed ground-based vegetation information within the study periods. Besides, assessment of

vegetation changes in this area can be rarely validated due to the limitation of field data availability. In 2000, there was an investigation on land cover in the Seward Peninsula by the National Science Foundation-sponsored Arctic Transitions in the Land-Atmosphere System (ATLAS) project called "Arctic Climate Change, Substrate, and Vegetation." They began examining the land cover types in the Seward Peninsula including the Council site from 1999, and installed 15 grid stations for identification of various vegetation types in Council site (Figure 3.2). Moreover, in order to achieve continuous weather data, several weather stations were installed in diverse vegetated areas that are in a lowland tussock tundra area, near the top of a hill in the Melsing Creek area characterizing moss and lichen, and upland tundra area (ATLAS). Based on their field data, ATLAS project conducted the study on measurement of vegetation properties in the Seward Peninsula using both ground data and remote sensing data. It was found that Council consisted of three dominant vegetation types that were open white spruce forest, low and tall shrub, and tundra areas, and these main vegetation types were distributed in terms of different elevation of the Council area. As described in Figure 3.3 and Table 3.1, *Picea glauca* (white spruce forest) is found along the upland area and mountain region mainly located between 50 m and 150 m in elevation. Average height of white spruce forest is 6.1 m and distributed with a density of 1,100 trees ha^{-1}. The lower-elevated regions between 30 m and 50 m contain a fairly uniform vegetation community of hummocks with lichens, dwarf shrub, and sedges (mostly tundra species). Shrubby woodlands such as low-shrub tundra and graminoid tundra are distributed relatively higher elevation sites between 150 m and 400 m in elevation in Council area. Most of shrub site consists of two different species that are tall deciduous shrub with a height of

greater than 1.5 m and low deciduous shrub such as *Betula glandulosa* and *Salix glauca* with a moss groundcover (Lundberg and Beringer 2005).

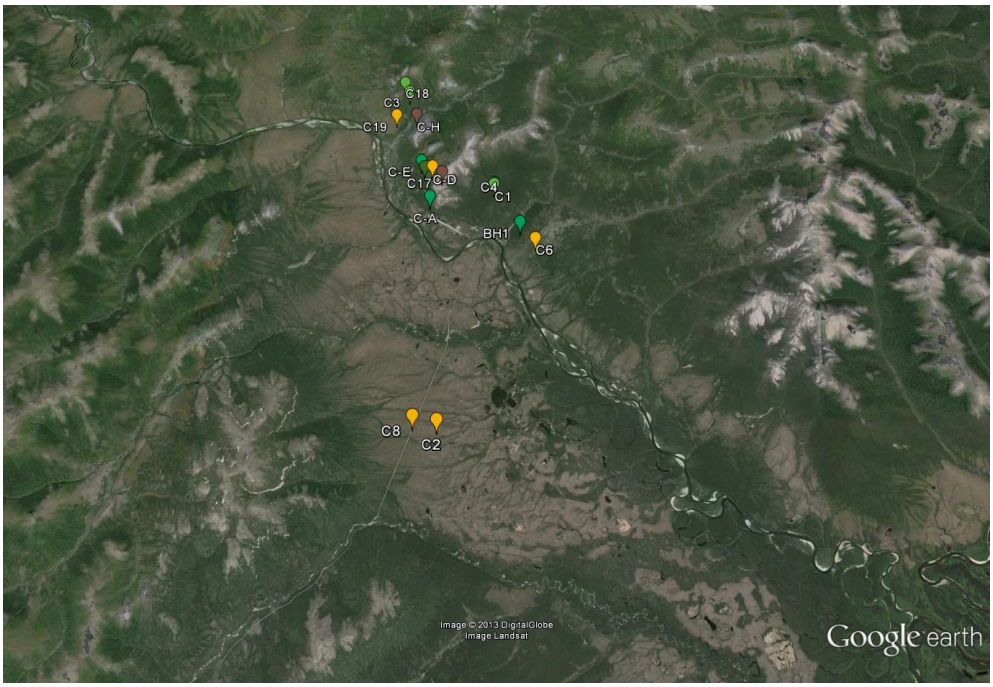

Figure 3.2 : Location of grid stations in Council Creek represented by different colors on Google Earth (dark green: forest area, green: shrub, yellow: tundra, and brown: dry tundra) and the coordinates of the location were derived from the ATLAS (http://www.eol.ucar.edu/projects/atlas/).

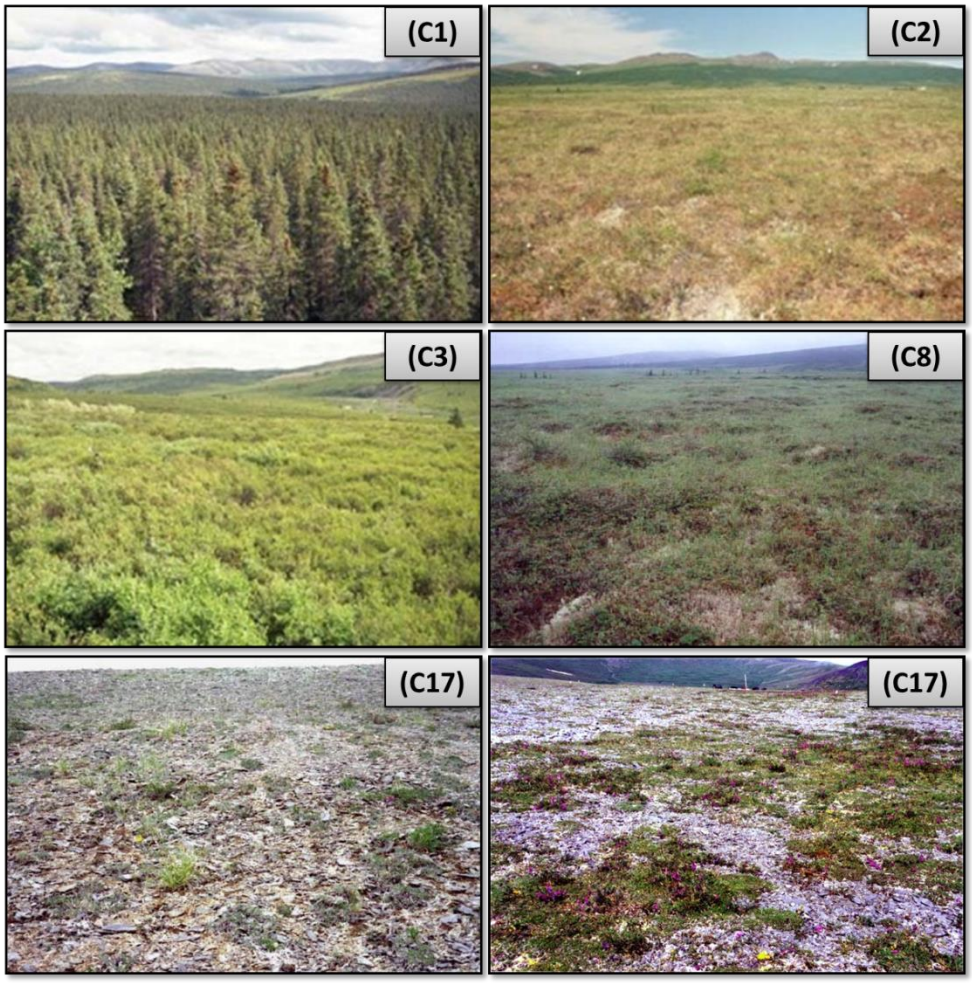

Figure 3.3 : Vegetation types found in the study area at grid stations. (C1): open white spruce forest site, (C2): tundra site identified in flat basin area, (C3): low and tall shrub site, (C8): dwarf-shrub and moss tundra site, and (C17): dry tundra site representing rocky limestone scree, images were provided from ATLAS (http://www.eol.ucar.edu/projects/atlas/).

Table 3.1: A summary of the dominant vegetation in the study area and the information was provided by the International Arctic Research Center (IARC) at the University of Alaska Fairbanks (http://www.iarc.uaf.edu/).

Region	Latitude/ Longitude	Elevation	Site	Description	Plant Community
C1	64.077/ 163.6748	45 m	Forest site Council, Seward Peninsula	▪ Open white spruce/willow forest. Successional forest with even aged Picea glauca ~ 10-15 diameter.	Moist *Picea glauca*, Salix species, *Vaccinium uliginosum*, *Hylocomium splendens*, evergreen tree, low-shrub forest
C2	64.8418/ 163.6930	43 m	Tundra site 10km west of Council, Seward Peninsula	▪ Flat basins dissected by several small drainages. ▪ Interfluves – flat, hummocky with lichens, dwarf shrubs and sedges.	Moist *Rubus chamaemorus*, *Betula nana*, *Ledum decumbens*, *Sphagnum fuscum* erect dwarf-shrub, moss
C3	64.8418/ 163.7357	86 m	Shrub site Ophir Creek, Council, Seward Peninsula	▪ Shrubs on 5° slope, east side of creek. ▪ Dominated by *Betula Glandulosa* and willows.	Moist *Betula glandulosa*, *Salix glauca*, *Hylocomium splendens* low-shrub tundra, graminoid tundra
C4	64.9074/ 163.6750	40 m	Shrub woodland Council, Seward Peninsula	▪ Open woodland with low shrubs on hill above Melsing Creek.	Moist *Salix pulchra, Betula glandulosa*, *Picea glauca* low-shrub woodland
C6	64.8919/ 163.6470	113 m	Moist tundra site Blueberry Hill, Council, Seward Peninsula	▪ Broad hillslope on shale derived collucium. ▪ Moist tundra on 10° slope to west 1.5km south east of Council.	Moist *Betula nana*, *Ledum decumbens*, *Vaccinium uliginosum*, *Carex bigelowii*, *Sphagnum* species, lichen dwarf shrub tundra
C8	64.8423/ 163.7064	54 m	Hummock tundra 10 km west of Council, Seward Peninsula	▪ Slight slope to southeast with shrubby drainages.	Moist *Rubus chamaemorus*, *Empetrum nigrum*, *Vaccinium*

					uliginosum, *Sphagnum russowii* dwarf-shrub, moss tundra
C17	64.9093/ 163.7076	223 m	Dry tundra site Council mountain, Seward Peninsula	▪ Rocky scree near top of Council Mountain. ▪ 60 % rocky limestone scree.	Dry *Dryas octopetala*, *Hedysarum mackenzii*, *Cetraria spp.*, *Thamnolia subuliformis prostrate* dwarf-shrub, forb, lichen barren
C18	64.9383/ 163.7394	114 m	Shrub site Ophir Creek, Council, Seward Peninsula	▪ Alders north of Ophir Creek.	Moist *Salix glauca*, *Pentaphylloides floribunda*, open low-shrub, graminoid, forb meadow
C19	64.9276/ 163.7418	76 m	Tussock tundra Ophir Creek, Council, Seward Peninsula	▪ Shoulder of broad hill slope north of Ophir Creek.	Moist *Eriophorum vaginatum*, *Rubus chamaemorus*, dwarf-shrub, tussock tundra
BH1	64.8965/ 163.657	55 m	Forest site Council, Seward Peninsula	▪ Forest north facing hill on south side of Melsing Creek.	Moist *Picea glauca*, *Betula glandulosa*, *Vaccinium uliginosum*, *Hylocomium splendens* low-shrub woodland
C-A	64.9021/ 163.7132	70 m	Forest site Council mountain, Seward Peninsula	▪ Spruce forest above and below Ophir Creek Road, near Council Mountain trail.	Moist *Picea glauca*, *Salix lanata*, *Alnus crispa* open needle leaf forest
C-C	64.911/ 163.7189	150 m	Shrub site Council Mountain, Seward Peninsula	▪ Low-shrub on south west side of Council Mountain.	Moist *Betula glandulosa*, low-shrub tundra
C-D	64.911/ 163.714	220 m	Tundra site Council Mountain, Seward	▪ *Equisetum* areas and/or probably snow accumulation	Moist *Equisetum arvense*, *Salix reticulata*, *Salix*

			Peninsula	area.	*lanata*, open low-shrub, dwarf-shrub, moss tundra
C-E	64.9129/ 163.7216	170 m	Forest site Council Mountain, Seward Peninsula	▪ 70% rocky limestone scree, 7 °slope to south.	Moist *Picea glauca*, *Alnus crispa*, woodland, low-shrub tundra
C-H	64.9281/ 163.729	80 m	Dry tundra site Council Mountain, Seward Peninsula.	▪ Maintain side ▪ North spur of Council Mountain, above Ophir Creek.	Dry *Dryas integrifolia*, *Cetraria* spp. prostrate dwarf-shrub, lichen tundra

According to pre-conducted study, four different vegetation categories were found within the study area, in the vicinity of Council region. Spruce forest was usually located 50 m above sea level and grew roughly below 300 m. Mostly white spruce (moist *Picea glauca*) mixed with evergreen trees and shrub were dominant in the spruce forest region. Shrubby sites were predominantly occupied by *Salix glauca* and *Hylocomium splendens* (upland, tall or low shrub) and the understory vegetation cover consisted mostly of grasses followed by mosses and lichens. These mosses and lichens were the dominant species in tundra areas. Depending on the moist condition and elevation, tundra areas could be characterized by two different regions: moist tundra and dry tundra. Most of moist tundra areas were covered by moist tussock graminoid, dwarf-shrub tundra, and lichen tundra, and drier tundra areas were occupied by dry *dryas octopetala*, *dryas integrifolia*, and yellow lichen tundra.

Chapter Four: DATA AND ANALYSIS METHODS

As explained in the objectives of this study, this study traces changes in vegetation over a ten year periods in Council, Alaska using remote sensing images. The results are expected to produce the time-series NDVI maps with NDVI and change detection techniques for showing changes in the area of vegetation density. The general work flow of the method used in this study is shown in Figure 4.1. This chapter contains the sections from the data acquisition to the final image processing. Two different types of data were collected in this study: remote sensing data and meteorological data. Landsat imagery was used as the main dataset and meteorological data were utilized to explore the relations between the vegetation changes and the climate conditions. The detailed methods used for the analysis will be explained.

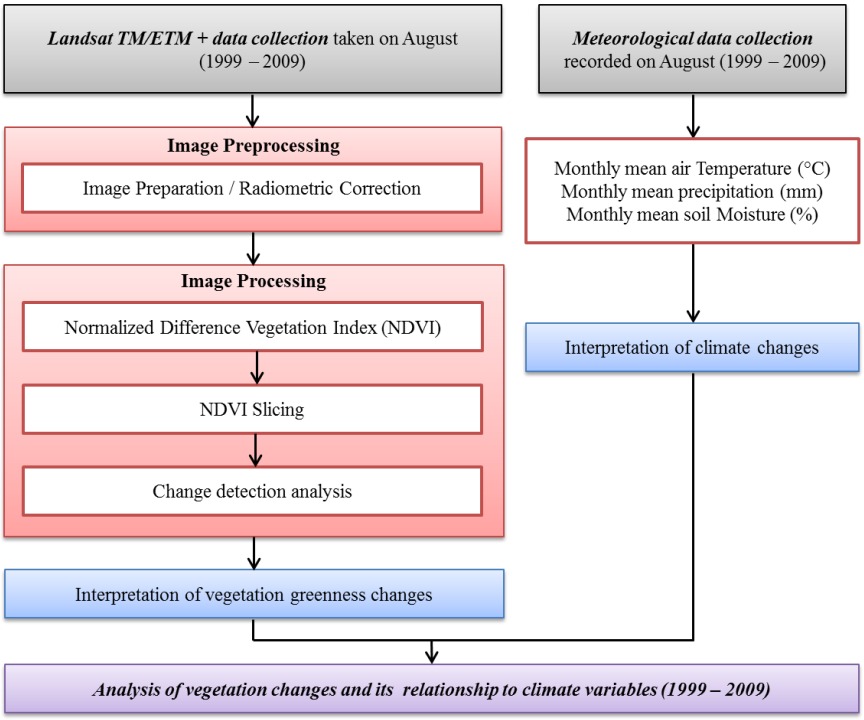

Figure 4.1 : Work flow of the detailed methods used in this thesis.

4.1 Data Acquisition

4.1.1 Satellite data acquisition

The Landsat TM and ETM+ imagery

Landsat images were selected as a primary data because of long-period data availability and medium spatial resolution which is helpful for mapping at regional scales (Xie et al. 2008). The images spanning from 1999 to 2009 were available in both Landsat TM and ETM+ sensors, and were obtained from the USGS National Center for Earth Resources Observation and Science (http://glovis.usgs.gov/). Table 4.1 provides a brief description of the two sensors that are TM and ETM+ available for this study. Two sensors offer 30 m spatial resolution and a large spectral window through the addition of several bands in the blue-visible, infrared and thermal spectrum (Xie et al. 2008).

Table 4.1 : Characteristics of Landsat TM and ETM+ sensors (Bruce and Hilbert 2004).

Sensors	Thematic Mapper (TM)	Enhanced Thematic Mapper Plus (ETM+)
Platform	Landsat 5	Landsat 7
Geographic Reference system	WRS-2 Paths: 233 Rows: 248	WRS-2 Paths: 233 Rows: 248
Orbit	16 day / 705 km	16 day / 705 km
Inclination	98.2°	98.2°
Swath width	185 km	185 km
Bands	1 (0.45 – 0.52 µm) 2 (0.52 – 0.60 µm)	1 (0.45 – 0.52 µm) 2 (0.52 – 0.60 µm)

	3 (0.63 – 0.69 µm) 4 (0.76 – 0.90 µm) 5 (1.55 – 1.75 µm) 6 (10.4 – 12.5 µm) 7 (2.08 – 2.35 µm)	3 (0.63 – 0.69 µm) 4 (0.76 – 0.90 µm) 5 (1.55 – 1.75 µm) 6 (10.4 – 12.5 µm) 7 (2.08 – 2.35 µm) Panchromatic band 8 (0.50 – 0.90 µm)
Ground pixel size	30 m (bands 1 – 5, 7) 120 m (band 6)	30 m (bands 1 – 5, 7) 60 m (band 6) 15 m / 18 m (band 8)
Quantisation levels	8 bits	Best 8 of 9 bits

Five images, listed in Table 4.2, were selected between 1999 and 2009 from mid to late August, when snow cover is at its annual minimum. All imagery was obtained using level 1T processing (Table 4.3).

Table 4.2 : Landsat imagery used in the study.

Sensors	WRS Scene	Acquisition Dates
Landsat 7 ETM+	Path 79 Row 15	1999/08/29
Landsat 7 ETM+	Path 79 Row 15	2002/08/21
Landsat 7 ETM+	Path 79 Row 15	2004/08/26
Landsat 5 TM	Path 79 Row 15	2006/08/31
Landsat 5 TM	Path 79 Row 15	2009/08/16

Table 4.3 : Obtained USGS Landsat Level 1T imagery information (Landsat Science Team 2010) from the USGS-Landsat website (http://landsat.usgs.gov).

LPGS parameter	Description
Datum	WGS-84
Projection	Universal Transverse Mercator (UTM)
Map orientation	North up
Distribution format	8 bit unsigned GeoTIFF
Pixel Size	TM and ETM+ : 30 metre (bands 1 – 5, 7)
Resampling method	Cubic Convolution (CC)
Correction Level	Standard Terrain Correction (Level 1T) – provides systematic radiometric and geometric accuracy by incorporating ground control points while employing a Digital Elevation Model (DEM) for topographic accuracy. Geodetic accuracy of 25 to 30 meters by use of ground control points (GCP) and terrain correction using DEM.

4.1.2 Meteorological data acquisition

Meteorological data were provided from the International Arctic Research Center (IARC) at the University of Alaska Fairbanks (http://www.iarc.uaf.edu/). The meteorological data were collected in a C1-grid Station (Figure 4.2) located at 64°50.60´N and 163°42.32´W about 50 m above sea level. In order to investigate the annual weather variations within the study years, hourly-based temperature, rainfall, and soil moisture data measured on August were obtained. The air temperature was measured hourly at a height of 3 m, and rainfall data were accumulated and expressed as hourly measurements with the unit of millimetres. In addition, the soil moisture content was sampled at this site and measured at six different depths (5, 10, 15, 20, 25, and 30 cm). A three-hour accumulated soil moisture value, expressed as a percentage of the water content, was used over the study

period. The attained hourly-based meteorological data were converted to mean and total monthly data for analysis.

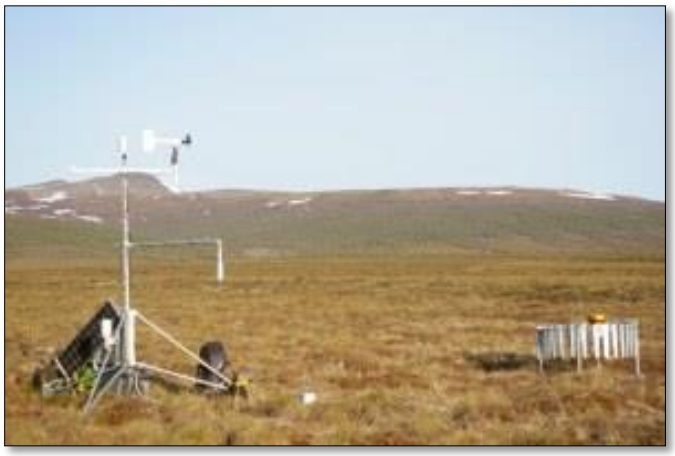

Figure 4.2 : Seward Peninsula C1 Grid site photo taken in June 2005 (http://ine.uaf.edu).

4.2 Software and Hardware

ERDAS Imagine 2011 and ArcGIS 10 were mainly used for image processing and interpretation. MATLAB was the chosen mathematical computation tool for the analysis of statistical data. These necessary software were installed on an Inter (R) Core (TM) i5-2310 CPU (64bit) with 8.00 GB RAM with a platform of Windows 7, which was tested for successful performance.

4.3 Image Pre-processing

Even though Landsat imagery is already corrected geometrically and radiometrically by obtaining Level 1T data, some pre-processing procedures are required before image processing such as NDVI and change detection. The following subsections will discuss the required image pre-processing procedures in detail.

4.3.1 Image preparation

Due to the failure of Landsat 7 ETM+ SLC on May 3, 2003, the obtained image taken in 2004 has striping lines, and it needs to be processed to fill the gaps. There have been several attempts to develop an algorithm for filling gaps in imagery, and this study adopted one of the methods provided by USGS using ERDAS Imagine (http://landsat.usgs.gov/ERDAS_Approach.php). This method is designed to adjust neighboring pixels in a single Landsat 7 SLC-off scene (Landsat Science Team 2010) and fills the gaps using interpolation of data by using mean function. The process is called a focal mean and it takes a 3 x 3 sample around the missing data in order to fill in the pixel with the result. This procedure was repeated until the gap was filled. This study performed this approach repeating more than five times and generated gap-filled results shown in Figure 4.3.

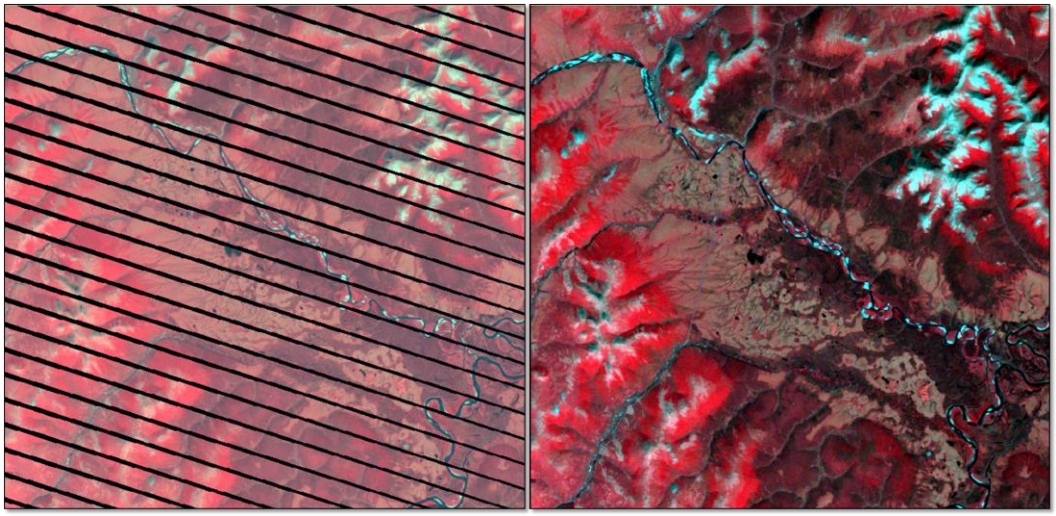

Figure 4.3 : Landsat 7 ETM+ imagery taken from 2003/09/25 (left) and corrected image with SLC data gaps and 5 focal mean functions applied (right), represented the study area (both images composite of R, G, and B: ETM+ 4, 3, 2 bands).

For the implementation of image processing, a six-layer stack for optical bands 1 through 5 and 7, corresponding to the visible and infrared regions, was created as a band-sequential format file. In addition, as the spatial extent of these stacked layers was much larger than the study area, the stacked layers were clipped into the specific boundary shown in a Figure 4.3.

4.3.2 Radiometric correction

Radiometric correction is a common preprocessing step when considering multi-temporal image processing. Changes in obtained imagery taken at different times occur because of the internal and/or external influences from the satellite sensors and atmospheric condition (e.g., surface condition, sun angle, earth-sun distance, detector calibration,

atmospheric condition, and sun-target-sensor geometry). This study performed atmospheric correction by adopting the absolute calibration of individual imagery for which the sensor characteristics, atmospheric conditions, and illumination angles are easily demonstrated (McDermid et al. 2005). Among the various calibration algorithms, corrections used in this study included the calculation of radiance units, at-satellite reflectance, and a histogram matching.

The conversion of radiance units and at-satellite reflectance compensate for differences in sun azimuth and elevation in order to diminish pixel brightness value variation by normalizing multi-temporal data. Digital numbers (DN) of all obtained Landsat data were scaled to radiance value using the following equation proposed by Chander and Markham (2003):

$$L_\lambda = \text{DN} \times \text{gain} + \text{bias}$$

L_λ is the spectral radiance detected satellite sensor, DN is the digital number of the sensor measurement, and gain and bias are sensor-specific calibration parameters shown in Table 4.4. Then, these at-satellite radiances were converted to at-satellite reflectance by correcting the solar effects using the following equation (Chander and Markham 2003):

$$\text{P}_{\text{surface}} = \frac{\Pi \cdot L_\lambda \cdot d^2}{ESUN_\lambda \cdot \cos\theta_s}$$

$\text{P}_{\text{surface}}$ is the unitless planetary reflectance, d is the earth-sun distance in astronomical units, $ESUN_\lambda$ is the mean solar exoatmospheric irradiances shown in Table 4.5, θ_s is the solar zenith angle in degrees (90 – solar elevation angle), and solar elevation angle is provided in a header file of the obtained image.

Table 4.4 : Post-calibration dynamic ranges for the acquired images (Chander and Markham 2003; Bruce and Hilbert 2004).

Spectral Radiances, Gain and Bias in $W/(m^2 \cdot sr \cdot \mu m)$						
Sensor	Landsat ETM+		Landsat TM 5 Before May 5, 2003		Landsat TM 5 After May 5, 2003	
Band	Gain	Bias	Gain	Bias	Gain	Bias
1	0.775686275	-6.2	0.602431	-1.52	0.7628235	-1.52
2	0.795686275	-6.4	1.175100	-2.84	1.4425098	-2.84
3	0.619215686	-5.0	0.805765	-1.17	1.0398824	-1.17
4	0.637254902	-5.1	0.814549	-1.51	0.8725882	-1.51
5	0.12572549	-1.0	0.108078	-0.37	0.1198824	-0.37
7	0.04372549	-0.35	0.056980	-0.15	0.0652941	-0.15

Table 4.5 : Solar exoatmospheric spectral irradiances for both TM and ETM+ (Chander and Markham 2003; Bruce and Hilbert 2004).

Units: ESUN = $W/(m^2 \cdot \mu m)$		
Band	**Landsat TM 5**	**Landsat 7 ETM +**
1	1957	1969
2	1826	1840
3	1554	1551
4	1036	1044
5	215.0	225.7
7	80.67	82.07

Chander and Markham (2003) stated that there are two advantages to using reflectance instead of radiance when comparing images from different sensors. First, the cosine effect of different solar zenith angles due to the time difference between the data

acquisitions can be removed, and it compensates for different values of the exoatmospheric solar irradiances arising from the spectral band differences.

Moreover, obtained data need to be calibrated atmospherically due to atmospheric scattering since water vapour and aerosols can induce variations in reflectivity between images. This study selected a histogram matching method as a relative atmospheric correction to remove the disturbing effects on the image. The idea behind this method is quite simple and easy to implement. This approach provided by ERDAS Imagine software implements the calibration automatically by matching the servant image to the master image. For the process, the Landsat 5 TM image taken in 2009 showing relatively clear atmospheric condition was selected as a master image and other images (e.g., servant images) were used to be matched to the master image. Since the obtained Landsat images were covering the same land surface and were taken in August, it is assumed that the general shape of the histogram curves of the images are similar, and relative dark and light objects in images are also same (ERDAS 1999). For the calibration, histogram matching uses the whole image area as a references area. The results of histogram before and after the matching are shown in Figure 4.4. According to the results, the calibrated histograms corresponded to the master image.

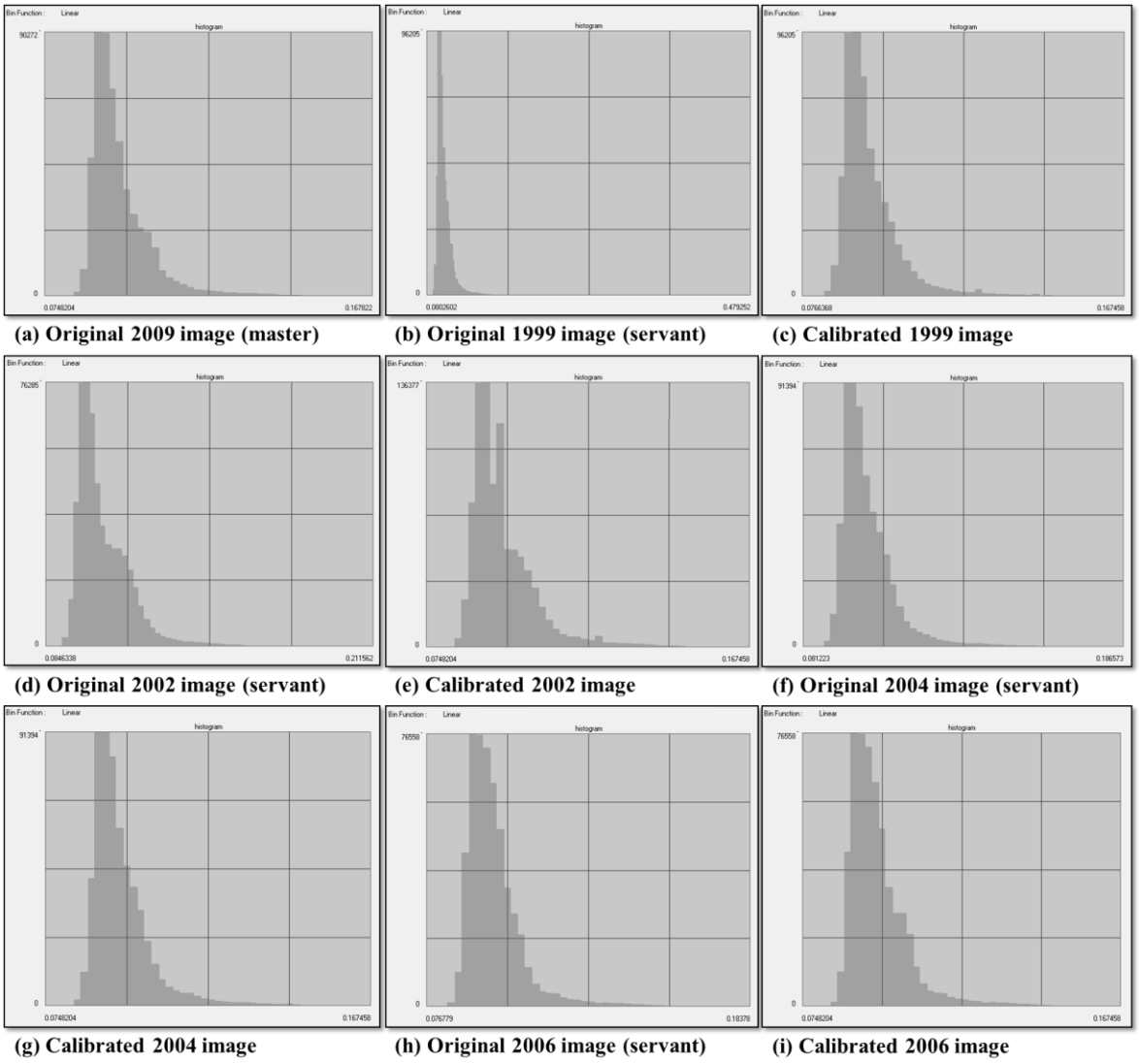

Figure 4.4 : Histograms of the images band 4 (near-infrared) with the master and servant images processed by histogram matching. X axes are reflectance value, and Y axes are number of pixels.

4.4 Image Processing

This section describes the various image processing steps required to produce the products to be analyzed for change detection. There are calculation of NDVI and determination of appropriate class breaks based on NDVI histogram. This will be followed by change analysis itself.

4.4.1 NDVI and Density Slicing

The NDVI was computed for each date image using bands 3 and 4 as input to detect vegetation density. In this manner, a total of five NDVI maps were generated. As simply looking at histogram of NDVI values, there were no obvious division points to classify vegetation categories. Thus, in order to decide the same division points for all NDVI results, temporary division points of each NDVI result were decided using Natural breaks (Jenks) algorithm provided by ArcGIS software. This method maximizes the differences between classes. The features are categorized into different classes by inserting divisions where there are relatively big jumps in the data values, if such jumps exist (ArcGIS 2007). NDVI was sliced using 6 classes, one each for water and glacier/snow, and four vegetation classes. This number of class was selected based on published ground mapping in the area (e.g., Lundberg and Beringer 2005; Beringer et al. 2005). Table 4.6 shows classified NDVI break points from NDVI results by Jenks method, and it is clearly indicated that all the class break points resulted in the similar values.

Table 4.6 : Break points (upper boundary) of the NDVI results computed by Natural breaks (Jenks) algorithm.

Date / Legend	1999/08/29	2002/08/21	2004/08/26	2006/08/31	2009/08/16
Class 1	0.14	0.17	0.16	0.14	0.14
Class 2	0.36	0.39	0.39	0.38	0.37
Class 3	0.50	0.52	0.52	0.52	0.51
Class 4	0.59	0.59	0.60	0.60	0.60
Class 5	0.67	0.67	0.68	0.68	0.67
Class 6	0.81	0.81	0.82	0.81	0.81

To use the same break points of NDVI values for the NDVI slicing, the break points were averaged and relocated into these calculated new division points. New division points (upper boundary) are 0.15, 0.38, 0.51, 0.6, 0.67 and 0.82. The first two classes ranging from -0.55 to 0.38 were later collapsed excluded from analysis, as this interval is indicative of little or no vegetation such as water and glacier/snow regions. The four remaining classes from 0.38 to 0.82 were categorized by the different name of classes (e.g., spruce forest, shrub, moist tundra, and dry tundra) depending on NDVI values. Then, area (m^2) and % total area for the four classes were calculated.

4.4.2 NDVI change detection

Successive pairs of images (e.g., 1999 – 2002 and 2002 – 2004) were subtracted from one another. In this way, changes for each two-year period were calculated. Each difference image was output indicating % change, and these were grouped into five categories: decrease (changes more than 10 %), increase (changes more than 10 %), less decrease

(changes less than 10 %), and some increase (changes less than 10 %), and unchanged (changes less than ± 1 %) areas. Therefore, the outcomes represented the areas where the vegetation greenness has increased or decreased. The multi-date NDVI results were compared visually in four intervals: 1999 to 2002, 2002 to 2004, 2004 to 2006, and 2006 to 2009.

Chapter Five: RESULTS AND DISCUSSION

5.1 NDVI results

5.1.1 Satellite-driven NDVI maps

The time-series NDVI results were derived from the obtained Landsat images for analyzing the vegetation changes within the study period. The computed NDVI ranged from -0.5 (corresponding to likely low-reflectance areas such as water and glacier regions) to 0.8 (corresponding to the most highly vegetated areas). The NDVI results were then sliced to highlight the changes on each vegetation type. The outcomes are presented in Figure 5.1 that is highly matched to previously conducted classification result by ATLAS project. A total of five NDVI classes were created and assigned mapping colors: dry tundra (brown), moist tundra (yellow), spruce forest (dark green), and low and tall shrub (green); non-vegetation areas are shown in black. The idea behind the characterization of NDVI classes is that NDVI is significantly influenced on the forest canopy fraction and vegetation chlorophyll content. Lower NDVI would be expected in dry tundra areas that have the least amount of leaves and low chlorophyll, and intermediate NDVI would be identified in evergreen forests having a moderate leaf surface (needles) with a moderate chlorophyll content. Higher NDVI would be expected in a large amount of leaf area and chlorophyll content for deciduous areas like shrubs and tall shrubs (Simms and Ward 2013).

Low NDVI can be seen in the little-vegetation area identified as dry tundra region where it is close to the glacier and near flat basin. Similarly, water and glacier areas have NDVI values lower than 0.38. Higher NDVI values appear near the uplands and rivers that are mostly identified as spruce forest and shrub sites. Overall, spruce forest covered the most area and especially was distributed over the mountainous area in the east part of the Council region, which is called the White Mountain region. Moreover, spruce forest (e.g., woodland) can be found even in the flat basin and along the river. Highest NDVI areas (0.67 – 0.82) that are low and tall shrub sites mainly can be seen in the west part of the Council area where the elevation is lower than the forested area. Some shrub can also be found in the vicinity of forested area. Moist tundra is generally distributed in the flat basin and near valley and dry tundra can be seen mainly close to glacier. However, dry tundra having lower NDVI values than moist tundra area can also be found near the moist tundra region depending on the moisture condition as the moist and dry tundra are distinguished by its moisture content of tundra (Oberbauer et al. 2007).

In accordance with the sliced-NDVI maps presented in the chorological order of the data acquisition year (Figure 5.1), there are minor differences in the locations of all the vegetation classes. For example, more moist tundra areas appeared in the mountainous areas in the years of 2002 and 2006 and less dry tundra areas were identified in the flat regions in the years of 2004 and 2006. However, there do not appear to be any extensive changes that occurred in the 10 years of the study.

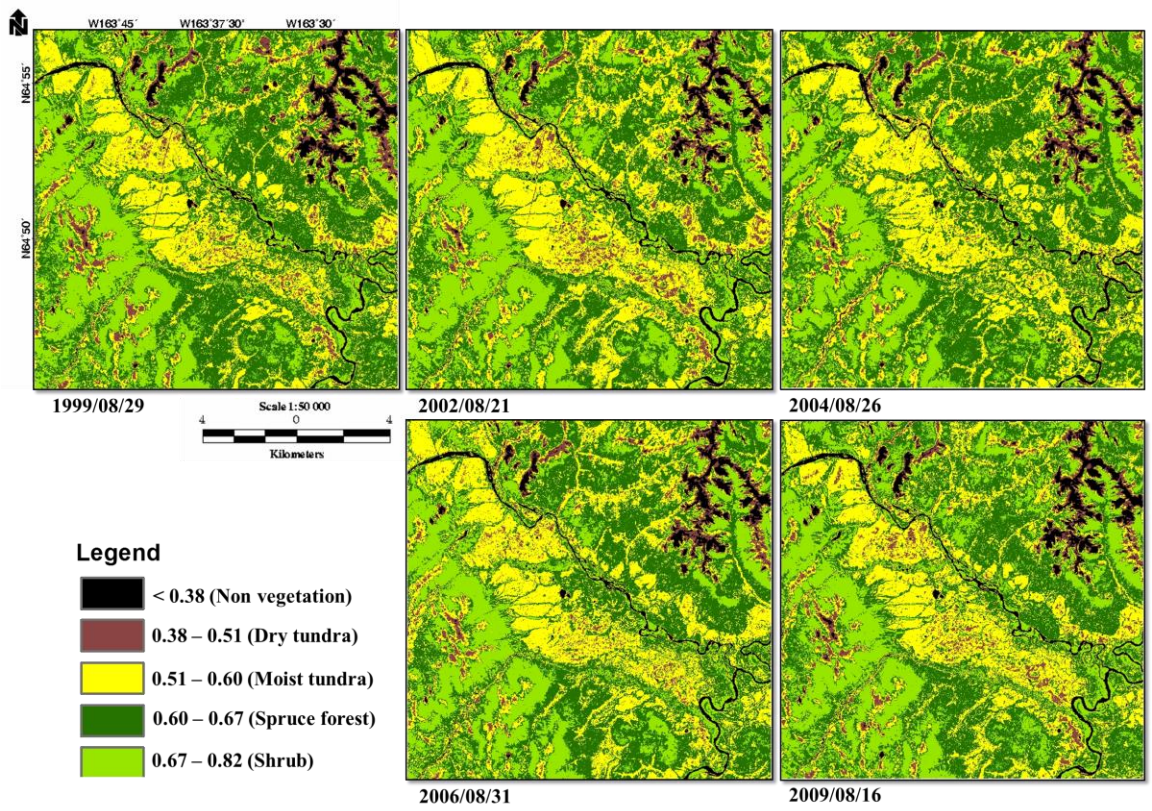

Figure 5.1 : The results of classified NDVI maps in the study area from 1999 to 2009 in August.

5.1.2 Statistics of classified NDVI results and Interpretation

For the detailed interpretation of vegetation changes, class statistics for the vegetation classes were computed and presented in Table 5.1. The trend of changes in the area of vegetation feature was also analyzed using the linear trend line and graphically visualized in Figure 5.2. According to the statistical results and the trend line graphs, the class with the largest area (almost 39 %) was spruce forest with the NDVI value ranging from 0.60 to 0.67 within the study period. More than half of the total area was occupied by moist tundra and shrub (NDVI ranges from 0.51 to 0.67) whereas the lower NDVI range from

0.38 to 0.51 (dry tundra areas) was more rare in the study area. Across all the five years, a total percentage of vegetation area has not been changed greatly in the NDVI range from 0.38 to 0.82.

Table 5.1 : NDVI changes on different ranges within the study period.

Vegetation type	NDVI range	1999/08/29	2002/08/21	2004/08/26	2006/08/31	2009/08/16
		Area (%)	Area (%)	Area (%)	Area (%)	Area (%)
Dry tundra	0.38 – 0.51	7.11	6.61	5.43	5.97	6.80
Moist tundra	0.51 – 0.60	26.16	30.74	29.14	30.48	27.53
Spruce forest	0.60 – 0.67	40.05	35.63	44.07	39.58	37.66
Shrub	0.67 – 0.82	22.41	23.19	17.76	20.08	23.45
TOTALS		95.73	96.17	96.40	96.11	95.44

As demonstrated in Figure 5.2, generally all NDVI ranges showed fluctuations in percent area within the study period. The ranges in 0.38 – 0.51 (i.e., dry tundra area), 0.60 – 0.67 (i.e., spruce forest area), and 0.67 – 0.82 (i.e., shrub area) showed a decreasing trend from 1999 to 2009 in the linear trend line. In contrast, the second range, 0.51 – 0.60, a moist tundra area increased in area. It can be explained that most of vegetation areas had decreased its size slightly within the study periods, except moist tundra areas. Despite the fact that linear trend line could provide the trend changes, there had been much fluctuation as showing the large differences in percent area between years in all vegetation types.

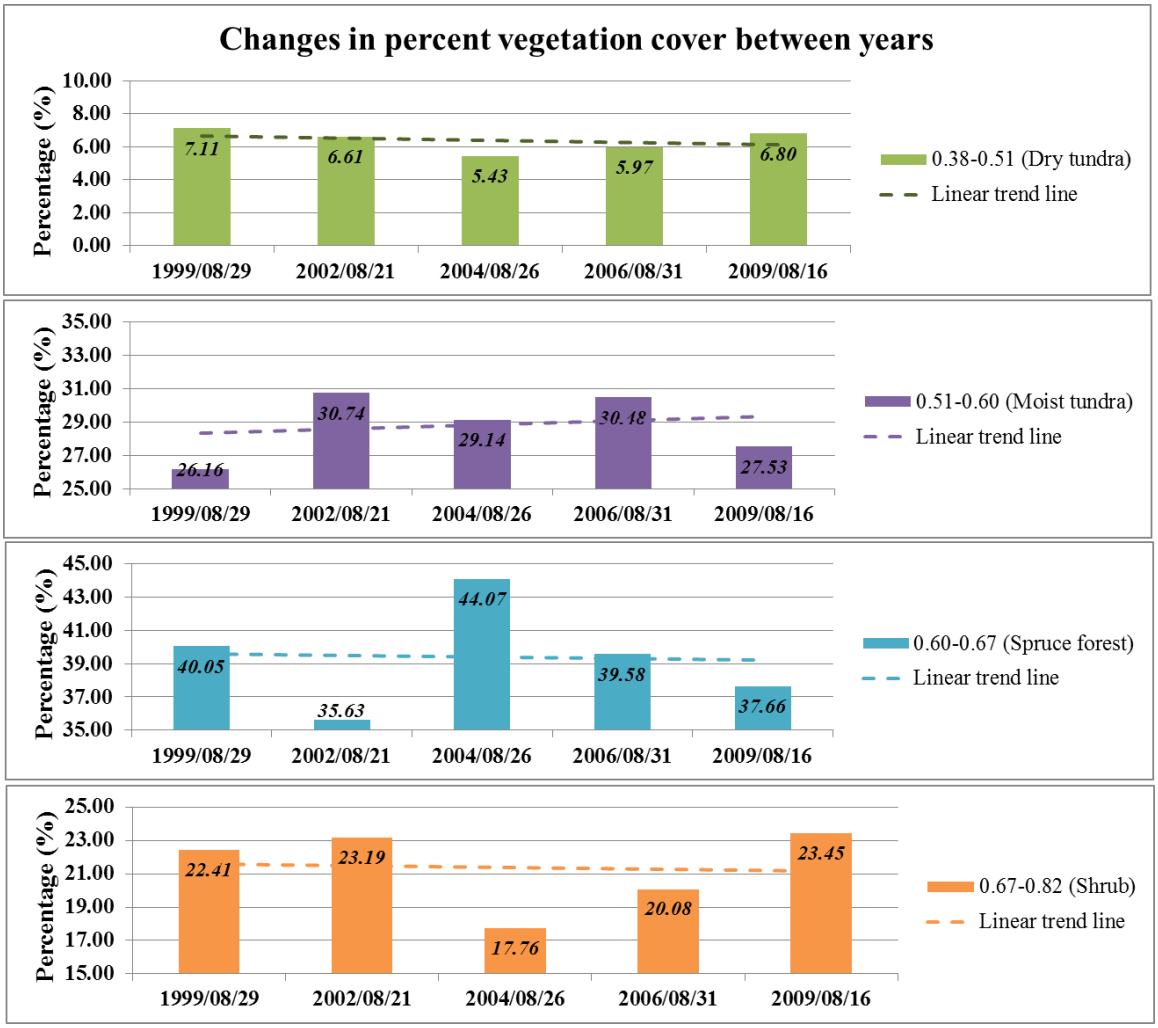

Figure 5.2 : Changes in percentage of vegetation area from classified NDVI results and linear trend line over the study periods.

In addition to the percentage changes in all NDVI ranges, the mean and maximum NDVI for the entire image were derived from the NDVI results to investigate how the overall vegetation greenness had changed for ten years. These results are visualized graphically with the linear trend lines in Figure 5.3. The mean and maximum NDVI had changed slightly between years, and overall there is a minor decreasing trend of vegetation greenness.

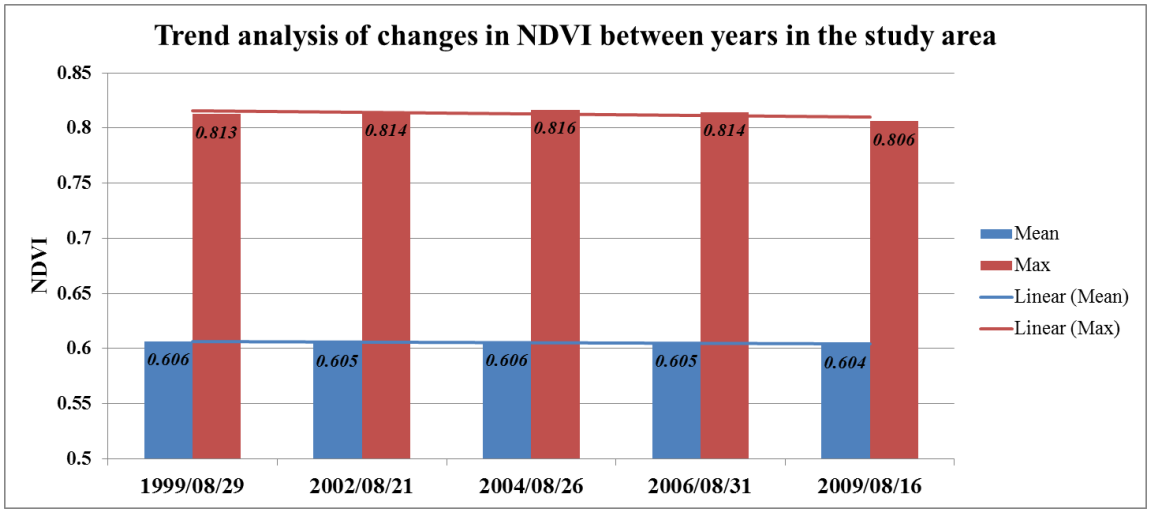

Figure 5.3 : Computed mean and maximum NDVI from Landsat-derived NDVI maps and linear trend line of NDVI changes over the study periods.

5.1.3 NDVI change detection

As discussed above, vegetation greenness had been changing in Council region over the study period. To compare how the vegetation had changed between two different years within the study period, the NDVI results acquired from different dates were examined by means of image differencing. Figure 5.4 demonstrates the NDVI differences between two successive images, delineating whether the NDVI had decreased or increased. The NDVI change detection map was subdivided into five categories: decreased and increased areas (change > ±10 %), less decrease and some increase areas (change < ±10 %), and unchanged areas (change < ±1 %). Since the analysis of changes in NDVI concentrated on vegetation areas, NDVI of non-vegetation areas (e.g., water and glacier areas) was masked out and shown as grey color in Figure 5.4.

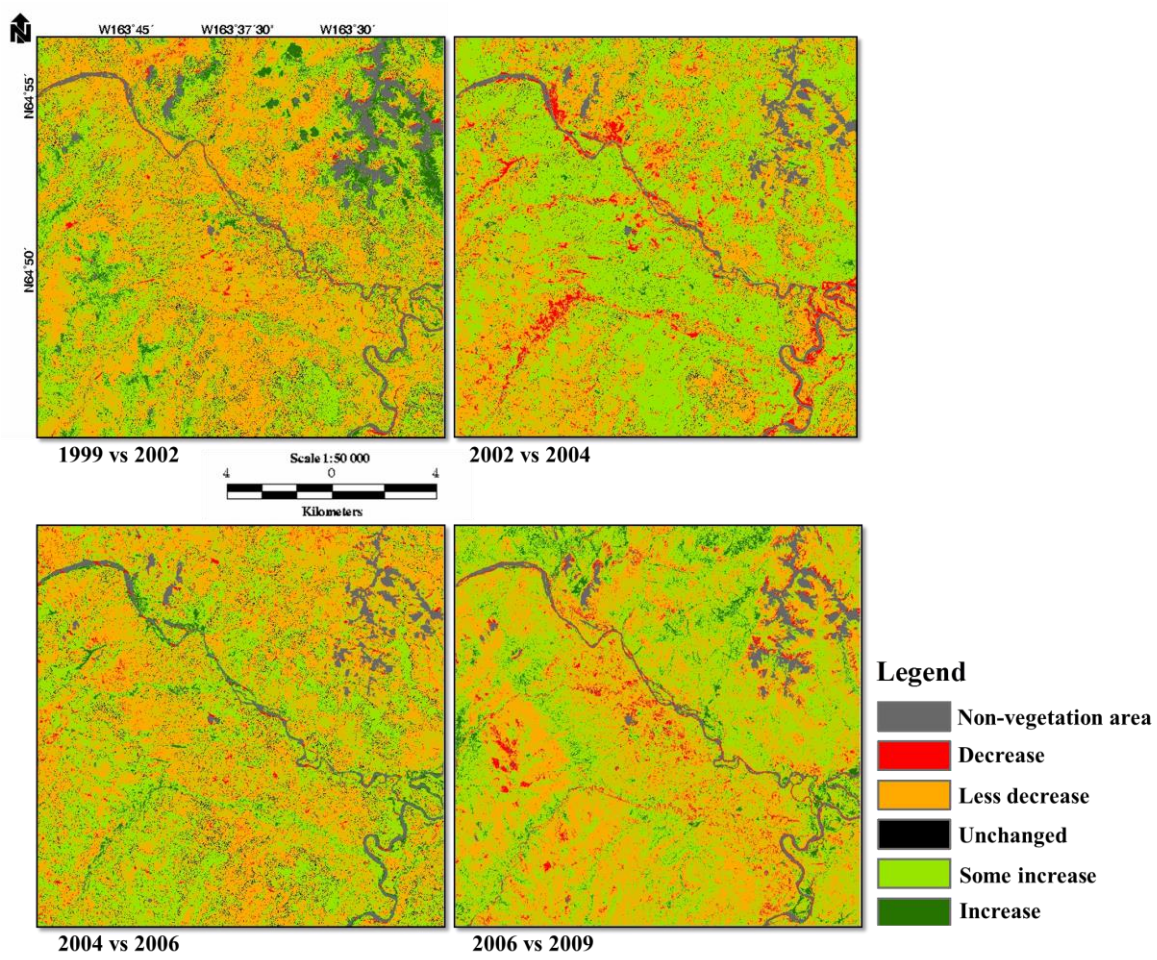

Figure 5.4 : NDVI change detection maps between data acquisition years.

It is clearly seen that the amount of changes of NDVI varies depending on the data acquisition years. The NDVI difference map between the years of 1999 and 2002 mostly appeared orangish color on relatively lower elevation area (flat basin and near valleys). The most of greenness near the moist tundra and spruce forest area close to the east part of the mountain declined from 1999 to 2002. In contrast, relatively higher elevation areas in the west part and near the top of the mountain which are mostly occupied by shrub and some of dry tundra showed increasing patterns of NDVI (greenish areas). For the years

between 2002 and 2004, the opposite changing pattern of greenness was found compared to the result between 1999 and 2002. The noticeable decline in the NDVI was focused mostly near the water region (river and valley) while the greenness increased in the vicinity of the moist tundra area and mountainous area from 2002 to 2004. Conversely, decreases in the NDVI were obvious near the flat basin and forested area in the east part of the study area between 2004 and 2006, but the NDVI increased exceptionally near the water region and some hill-sides of the western portion (shrubby site). From 2006 to 2009, the extreme decrease of greenness was found apparently in most of the tundra area where covers flat basin and near the top of the mountain. A noticeable decreasing trend was shown especially near the water region while some of moist tundra region in the upper-west part and forested areas showed increasing trend of NDVI.

Apart from the changes in the NDVI between 2002 and 2004, the similar changing pattern of vegetation greenness was identified in the change detection results as decreasing trend was shown in relatively low elevation area (near flat basin), and increasing trend was found in elevated area. This fluctuation indicates that vegetation greenness is likely to change year to year, and the phenomenon can potentially be explained by annual obtained meteorological data.

5.2 Climate Variables

5.2.1 Temperature

The monthly average temperatures recorded at the Council station from 1999 to 2009 are shown in Figure 5.5. The overall average in August within this period was 10.82°C. It is indicated that this area is generally cool during the summer. The temperature was recorded close to the average with the exception of 2004, 2005, and 2007 that are relatively high. There is a slight positive slope to the trend line, but given the short period it cannot be interpreted as a real trend.

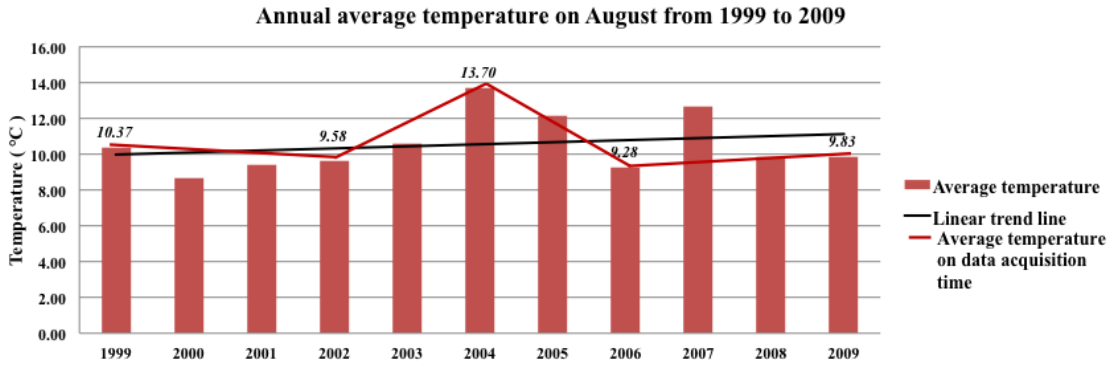

Figure 5.5 : Annual average temperature and linear trend line on August in Council, recorded at C1 site (64 ̊50.60 ̀N, 163 ̊42.32 ̀W).

5.2.2 Precipitation

The average of monthly total precipitation recorded in August at the Council station from 1999 to 2009 was 29.09 mm and the annual data are visualized in Figure 5.6. The rainfall varied unpredictably and was mostly below the average (less than 20 mm) but

considerably above the average in 2001, 2003, and 2004. From the measured data, four years from 2006 to 2009 were all extremely dry, at least in August. The linear trend line of rainfall shows a negative trend as opposed to the trend line of temperature data.

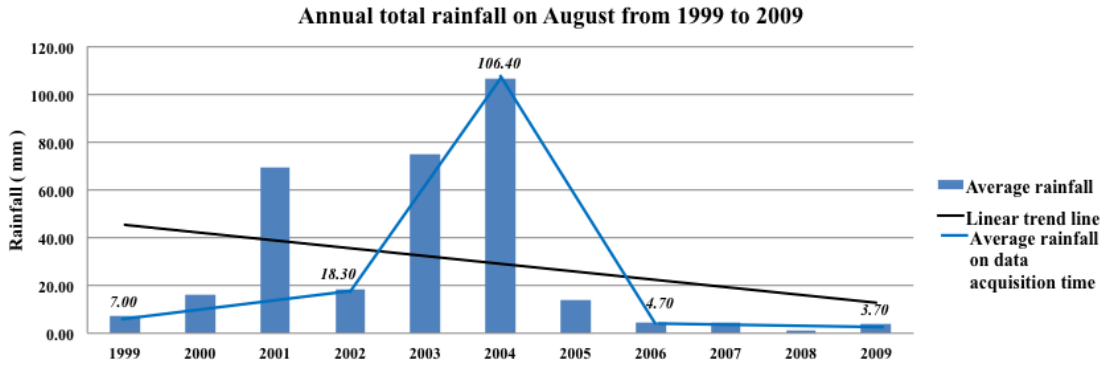

Figure 5.6 : Annual total rainfall and linear trend line on August in Council, recorded at C1 site (64 °50.60 'N, 163 °42.32 'W).

5.2.3 Soil moisture

The volume of water content (%) in the soil, so-called soil moisture, was recorded and the monthly total amount within the study period was computed. Figure 5.7 shows the monthly soil moisture accumulation and its linear trend line in August in the Council area. In accordance with the linear trend line, there is a slight negative trend similar to rainfall trend line. The observed soil moisture within the study periods closely followed the precipitation patterns, particularly between 2003 and 2004. Since 2005, a steady soil moisture level was observed.

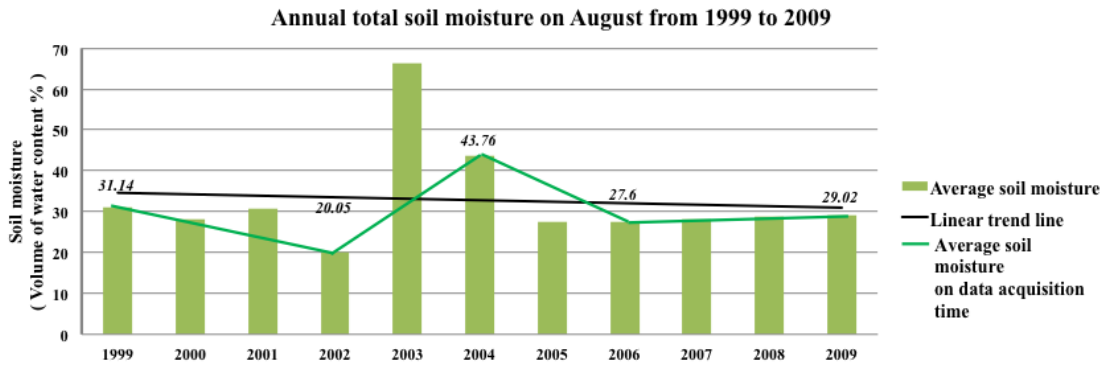

Figure 5.7 : Annual total soil moisture and linear trend line on August in Council, recorded at C1 site (64 ℃0.60 ℕ, 163 ℃42.32 ℠).

5.3 Discussion

Satellite-derived vegetation change analysis was developed for the 441 km^2 study area in Council, Alaska by the application of remote sensing technologies. Utilizing NDVI algorithm to multi-temporal images has been able to not only investigate the vegetation density changes over the study period but also relate the various NDVI slices to vegetation types in the area, although lack of timely ground data cannot support the accuracy assessment of the final step. The minimum NDVI values in NDVI results (Figure 5.3) occur when the years are relatively drying conditions (year of 2009). The maximum NDVI occur in 2004 when is the year with the highest temperature, the highest rainfall, and the highest soil moisture. Thus, it is predictable that the growth of vegetation communities in the study area may positively respond to higher temperature and moisture condition. In addition, the derived mean and maximum NDVI results (Figure 5.3) show a slight downward trend in NDVI. The decline in greenness of the study area as well as the

variation between successive years might result from several possible reasons, and the commonest causes of this change over a large area are climatic.

As discussed in Chapter 2, changes in Arctic vegetation were mostly attributed to temperature and moisture variations. The meteorological data reported that temperature varied from year to year with a very slight but most likely insignificant upward trend (Figure 5.5). There were quite a few dry years according to rainfall and soil moisture data, with showing a downward trend within the period (Figures 5.6 and 5.7). Due to the short period of the study year, there does not appear continuous meaningful trend, and rather the weather variables fluctuated every year of the study. This fluctuation may be related to inter-annual vegetation changes. It was expected that this noticeable local fluctuation in climate would lead to vary NDVI in each vegetation category (Figures 5.4) and would potentially affect the vegetation change particularly in grasslands (e.g., moist tundra and dry tundra). Therefore, the vegetation changes needed to be discussed in response to changes in the weather variables. Table 5.2 supports the comparison of changes in the weather variables and vegetation changes of each vegetation type for the interval year of two satellite acquisition dates. The interrelationships among these changes based on each vegetation characteristics will be discussed in following.

Table 5.2 : Comparison of climate changes to the vegetation changes for interval year of two satellite acquisition dates.

Climate variables	**1999 – 2002**	**2002 – 2004**	**2004 – 2006**	**2006 – 2009**
Temperatures	−*	+ +*	− −*	+*
Rainfall	+ +	+ +	− −	−
Soil moisture	− −	+ +	− −	+
NDVI changes	**1999 – 2002**	**2002 – 2004**	**2004 – 2006**	**2006 – 2009**
Dry tundra (0.38-0.51)	− 0.5 %	− 1.18 %	+ 0.54 %	+ 0.83 %
Moist tundra (0.51-0.60)	+ 4.58 %	− 1.6 %	+ 1.34 %	− 2.95 %
Spruce forest (0.60-0.67)	− 4.42 %	+ 8.44 %	− 4.49 %	− 1.92 %
Shrub (0.67-0.82)	+ 0.78 %	− 5.54 %	+ 2.32 %	+ 3.37 %

*− : less decrease (< 10%), − − : decrease (≥ 10%), + : some increase (< 10%), and + + : increase (≥ 10%).

The lowest NDVI indicated as dry tundra areas appeared less than 7 % of the study area that was seen in the higher topography (generally above 200 m) near the top mountain and in relatively drier area in tundra region (flat basin) (Figure 5.1 and 5.2). This low NDVI range (0.38 – 0.51) shows a slightly downward trend within the study period, and the percentage changes of its area appear to be closely related to the rainfall. The more rainfall increased, the smaller the area of this NDVI range (dry tundra) identified over a study period. It is presumed that dry tundra areas are vulnerable to changes in response to the moisture condition. As previous study conducted by Oberbauer et al. (2007) supported this observation by suggesting that the greatest production responses of dry tundra were found in low-precipitation regions. This NDVI range (dry tundra) may be directly affected by the amount of rainfall. Moreover, according to the changing pattern of dry tundra area and temperature (Figure 5.2 and 5.5), the area of lowest NDVI range

decreased when the temperature decreased under the relatively normal warm condition (i.e., the temperature close to the average). However, the smallest area was observed when the temperature is the extremely highest (the year of 2004). There may be possibility that the growth of dry tundra region (NDVI range of 0.38 to 0.51) can be constrained by higher-than-average warm condition.

The second range of NDVI (0.51 – 0.60) was recognized as moist tundra occupied a quite larger area than shrubby sites, showing that the overall average of this area was roughly 29 % (Table 5.1). The moist tundra within this range were generally seen in the regions of low topography (mostly located below 50 m), and some of them appeared above the shrub or spruce forest areas, which was close to the dry tundra region. Contrary to the downward trend of dry tundra regions, the moist tundra in the NDVI ranges between 0.51 and 0.60 showed an overall increasing trend (Figure 5.2) for study years. As shown in Table 5.2, the short-term response of the changes in moist tundra to the climate variables indicates that the moist tundra regions within the second NDVI ranges increased when the temperature and soil moisture decreased. This inverse relationship was shown by the investigation of the response of respiration of moist tundra to a warm temperature. Oberbauer et al. (2007) studied the tundra CO_2 fluxes in response to warm temperature in the Arctic and found that moist tundra responses were reduced by higher soil water content in warming condition because high soil moisture limits increases in respiration. Thus, the small detection of the areas in this NDVI range (moist tundra) may be mostly attributed by relatively warm and high moisture weather.

In addition, recent studies regarding the weather changes in northern Alaska (Mack et al. 2011; Gamon et al. 2013) reported that regional warm and dry condition was recently observed in many regions of the Alaskan North Slope over the past 30 years, resulting in shifting the tundra carbon balance. Increased temperatures tended to contribute to an early and longer growing season and resulted in thawing the Arctic permafrost and caused expansion of the tundra area (Stone et al. 2002). It was reported that the Council area had been identified as an area of discontinuous permafrost that had been experiencing thawing for a long time (Raynolds et al. 2008). When permafrost thaws, tundra wetlands and thermokarst lakes expand in area (Stone et al. 2002). As the NDVI range between 0.51 and 0.60 appeared near the wetlands especially in the vicinity of lakes in flat basin in Council, the slight upward trend in the area change of this ranges (moist tundra) might be triggered by many warm years and relatively steady lower moisture years recoded within the study period.

The higher NDVI ranges appeared in mostly spruce forest and shrubby sites. The NDVI ranges between 0.60 and 0.67 identified as spruce forest were dominant in the mountainous areas and along the rivers and occupied most of the study area (39 % on average) in accordance with the classified NDVI results (Table 5.1). As stated in the trend line analysis result (Figure 5.2), this NDVI ranges (spruce forest regions) showed a slight downward trend over the study years, but there may be no meaningful interpretation because spruce forests can hardly change within ten years due to the long lifespan. However, it can change the greenness (or biomass) year to year. Shown in Table 5.2, the area of this NDVI range fluctuated considerably between the years of 1999 and

2009. The interesting finding of the area change was that the changing pattern was highly related with local changes in the temperature and soil moisture showing positive relationship. The increasing NDVI in the spruce forest regions occurred in warm moisture years. In particular, the largest area in this range was observed when the temperature and moisture were the highest. In addition, continuous decreases in the area of this NDVI range appeared between 2004 and 2009. It may be greatly relevant to continuous decline in precipitation and soil moisture in these years. Known that evergreen needle leaf trees keep their leaves for many years, these trees (e.g., spruce forest) may also lose their leaves gradually and new leaves may be being grown for several years within the study period. Although spruce forest areas can barely diminish and increase for ten years, the growth of branches (needle) can influence on the variations in NDVI. As a result, the fluctuations of the NDVI range in spruce forest areas can possibly be prompted by higher temperature and higher moisture condition.

The highest NDVI (0.67 – 0.82) known as shrub areas and commonly found adjacent to the rivers and hillsides usually lower than spruce forest areas based on classified NDVI results (Figure 5.1). Unlike the changing pattern of the NDVI ranges in spruce forest areas, the area changes of this range between two different acquisition years decreased under the conditions of increased temperature and increased soil moisture (Table 5.2). When temperature and soil moisture were relatively higher than other years, less area of the highest NDVI range (shrub) was identified from the NDVI results. It is implied that shrub areas (the highest NDVI range) tend to be dense in relatively cooler and lesser moisture than too warm and high moisture conditions. According to both classified NDVI

results and weather change results (Figure 5.2, 5.5 through 5.7), the least shrub area (the smallest area of the highest NDVI range) was found in the warmest and the highest moisture year of 2004 as opposed to the result of spruce forest that appear the biggest areas in that year. Raynolds et al. (2008) supported the analysis that relatively lower elevation contains the wetter soil and shallower active layers, leading to limit the soil nutrient availability to the plant. Therefore, the growth of shrub (the highest NDVI vegetation communities) can be possibly grown in better-drained conditions.

5.4 Summary

A noticeable result was a slight downward trend in the overall mean and maximum NDVI over the study period. The decreases in the NDVI in the study area is another way of saying that decreases in vegetation greenness were observed, and this may have resulted from decreases in the vegetation areas that attain higher NDVI, mostly the range between 0.6 and 0.82 (possibilities of spruce forest and shrubby sites). Even though the linear trend lines of each NDVI range could not provide meaningful analysis due to the large variations between the years, the interesting fining is that there is a close relationship between inter-annual changes in the vegetation density and the inter-annual meteorological data changes over a ten-year period. The diverse ranges of NDVI fluctuated between two successive years and these variations were highly related to the temperature and the amount of soil moisture. It was expected that the warmer the area became, the greater greenness of vegetation that could be expected in general. However, the results contradict this indication, denoting an unexpected decrease in vegetation

growth in some of vegetation areas (moist tundra and shrubby sites with the NDVI ranges between 0.51 – 0.60 and 0.67 – 0.82) observed in the study area in the warm and moisture years. There were also differences in the vegetation growth between the dry and rainy seasons, and it was indicated that higher-than-average warm temperature and higher-than-average moisture condition might limit the growth of vegetation in this study area.

Chapter Six: CONCLUSIONS

6.1 Conclusions

Studying the ecosystem in the Arctic tundra region is considerably essential because of its large coverage of the earth's surface. Arctic vegetation has been undergoing various transitions depending on its regional characteristics. There are numerous contributors to the changes in Arctic vegetation, including direct human impact and natural changes in the earth's climate system. The commonest factor fostering the vegetation changes that are occurring is climate change. Due to the continual increases in temperature over the last 30 years in Alaska, degradation and alternation of vegetation communities have been appearing in various ways. In addition to the temperature increases, there are complicated external factors as we discovered, such as rainfall and soil moisture. Thus, the Arctic ecosystem needs to be closely examined and analyzed as it responds to climate change.

There is a variety of analyzing techniques, but remote sensing techniques have been able to provide exclusive observations into global vegetation growth patterns and changes that are promising as far as the data needed to quantify Arctic vegetation changes in the long term. In this thesis, Landsat TM and ETM+ imagery acquired between 1999 and 2009 in Council, Alaska during the greening season (August) were mainly utilized, not only to document the vegetation density changes but also to explore the relationship with the climate variables. Historical meteorological data were incorporated for the investigation to relate the inter-annual vegetation changes with inter-annual weather changes. As stated

that the Council area contained a diverse range of vegetation as a part of the Arctic tundra environment, advanced remote sensing techniques were required to analyze the changes. Unique methods therefore were applied in this study: the NDVI and change detection analysis.

The NDVIs derived from the obtained Landsat images provided greenness values for the unique types of vegetation in the study area and showed that the overall mean and maximum NDVI in the study area had been slightly decreasing since 1999. This result may be indicated that greenness of vegetation decreased in this area. In order to comprehensively examine the NDVI changes on the basis of different vegetation types, a density slicing method was performed on NDVI results by allocating the classes to known four vegetation features: spruce forest area, shrubby area, moist tundra and dry tundra areas. In spite of the lack of field data for the study area, the sliced-NDVI results provided the information on the unique vegetation areas and the non-vegetation areas (water and glacier). According to the results, the NDVI range between 0.60 and 0.67 identified as spruce forest areas occupied in the largest portion of the study area followed by moist tundra areas (the range between 0.51 – 0.60), low and tall shrubby sites (the range between 0.67 – 0.82), and dry tundra areas (the range between 0.38 – 0.51).

The outcomes were also used for change detection analysis. The low elevated areas (flat basin) with some of upland forested areas appeared decreases of NDVI over the study period except the years between 2002 and 2004. From 2002 to 2004, the opposite trend of NDVI changes was found, possibly resulting from extreme increasing temperature and

moisture condition recorded in 2004 in Council. In addition to this overall change, there have many fluctuations in the NDVI between two successive years. Both change detection and sliced-NDVI results allowed not only to trace back the trend of the vegetation density changes but also to examine in detail how the area of each NDVI range had changed year to year.

The observed variations on each NDVI range were closely related to local weather changes. As the vegetation characteristics of the NDVI ranges differ from each other, the response of the area change to weather variables varied. Most of the NDVI ranges (dry tundra, moist tundra areas, and shrubby areas) showed a negative relationship to the rainfall, and temperature and soil moisture, respectively, while the spruce forest areas (the range from 0.60 to 0.67) showed a positive relationship to temperature and soil moisture. As the Council area has relatively cool and less moisture summer, vegetation growth had not much changed under the cool and less moisture conditions. However, higher-than-average temperature and moisture conditions led to huge fluctuations in vegetation density. Therefore, the local weather variables may play an important role on the vegetation changes in Council area. The vegetation changes in the Arctic tundra environment can be examined utilizing long-term recorded satellite data by incorporating historical meteorological data to analyze possible causes.

Since the monitoring of vegetation changes for this study focused on regional scale observations of the Arctic tundra region, the observations from this study may not be representative of Arctic sites in general. Moreover, due to the lack of ground data, the

findings may not precisely explain the vegetation changes as this study relied on the historical remote sensing data and meteorological data. However, the outcomes derived from NDVI can be widely applicable where the area is characterized as Arctic tundra, especially the area of discontinuous permafrost region. The performed method accomplished the objective of this thesis by determining the vegetation density changes using appropriate spatial and temporal satellite data and successfully demonstrated differences with possible weather changes over ten years.

6.2 Limitations and Future Works

Some of the limitations of this study originate from the site-specific characteristics of the study area. As discussed, the study area (i.e., Arctic tundra) has limitations in acquiring adequate remote sensing data and performing precise research because of several factors:

- The relatively short growing season in this area hampers obtaining vegetation-peak season satellite data.
- Cloud cover can be seen persistently in Alaska regardless of the season, thereby limiting the availability of cloud-free imagery.
- Even during the summer season (July through September), consistent glacier and snow accumulation can be identified in the vegetation area.
- Due to similar vegetation species found in Alaska, detailed investigation of vegetation characteristics is challenging.

As aforementioned, obtainable ground truth is limited since this area is not fully accessible throughout the year. Access to the Council area is allowed during the short growing season only, which means that previously investigated research does not sufficiently support the generated results, causing difficulties in validation. As a result, the lack of ground data does not permit the assessment of change detection analysis.

In the future, collection of field data can verify the result and also provide the future assessment if possible. Other than Landsat data, the use of hyper-spectral data by taking advantage of a greater number of spectral bands enables more detailed vegetation studies. Although the NDVI successfully indicated the changes in vegetation greenness throughout the study period, utilizing other satellite-derived vegetation indices (e.g., tasseled cap transformation and leaf area index) could produce higher quality outcomes for identifying more sophisticated and detailed vegetation categories. In particular, a detailed investigation along with the biological aspects of vegetation is needed to provide more precise interpretation about climate change. Furthermore, supplementary investigations with respect to the external factors that foster vegetation changes are required in order to understand the observed changes.

Reference

ArcGIS (2007) ArcGIS Desktop Help 9.2 - natural breaks (jenks). In: ESRI. http://webhelp.esri.com/arcgisdesktop/9.2/index.cfm?topicname=natural_breaks_(jenks). Accessed 25 Mar 2014

ATLAS The Arctic Transitions in the Land-Atmosphere System (ATLAS) prject : Seward Peninsula Sites. http://www.eol.ucar.edu/projects/atlas/. Accessed 17 Apr 2014

Beck PSA, Kalmbach E, Joly D, et al. (2005) Modelling local distribution of an Arctic dwarf shrub indicates an important role for remote sensing of snow cover. Remote Sens Environ 98:110–121. doi: 10.1016/j.rse.2005.07.002

Berberoglu S, Akin A (2009) Assessing different remote sensing techniques to detect land use/cover changes in the eastern Mediterranean. Int J Appl Earth Obs Geoinformation 11:46–53. doi: 10.1016/j.jag.2008.06.002

Beringer J, Chapin FS, Thompson CC, McGuire AD (2005) Surface energy exchanges along a tundra-forest transition and feedbacks to climate. Agric For Meteorol 131:143–161. doi: 10.1016/j.agrformet.2005.05.006

Bruce CM, Hilbert DW (2004) Pre-processing methodology for application to Landsat TM/ETM+ imagery of the wet tropics. Cooperative Research Centre for Tropical Rainforest Ecology and Management. Rainforest CRC, Cairns, Qld.

Cakir HI, Khorram S, Nelson SAC (2006) Correspondence analysis for detecting land cover change. Remote Sens Environ 102:306–317. doi: 10.1016/j.rse.2006.02.023

Chander G, Markham B (2003) Revised landsat-5 tm radiometric calibration procedures and postcalibration dynamic ranges. IEEE Trans Geosci Remote Sens 41:2674–2677. doi: 10.1109/TGRS.2003.818464

Chen W, Blain D, Li J, et al. (2009) Biomass measurements and relationships with Landsat-7/ETM+ and JERS-1/SAR data over Canada's western sub-arctic and low arctic. Int J Remote Sens 30:2355–2376. doi: 10.1080/01431160802549401

Deering DW (1989) Field measurements of bidirectional reflectance. Theory and Applications of Optical Remote Sensing (G. Asrar, Ed.). Wiley 14-61

Dye DG, Tucker CJ (2003) Seasonality and trends of snow-cover, vegetation index, and temperature in northern Eurasia. Geophys Res Lett. doi: 10.1029/2002GL016384

Elmendorf SC, Henry GHR, Hollister RD, et al. (2012) Global assessment of experimental climate warming on tundra vegetation: heterogeneity over space and time. Ecol Lett 15:164–175. doi: 10.1111/j.1461-0248.2011.01716.x

ERDAS (1999) Erdas Field Guide. Erdas Inc., Atalanta, Georgia

Gamon JA, Huemmrich KF, Stone RS, Tweedie CE (2013) Spatial and temporal variation in primary productivity (NDVI) of coastal Alaskan tundra: Decreased vegetation growth following earlier snowmelt. Remote Sens Environ 129:144–153. doi: 10.1016/j.rse.2012.10.030

Giri C, Pengra B, Zhu Z, et al. (2007) Monitoring mangrove forest dynamics of the Sundarbans in Bangladesh and India using multi-temporal satellite data from 1973 to 2000. Estuar Coast Shelf Sci 73:91–100. doi: 10.1016/j.ecss.2006.12.019

Groisman PY, Karl TR, Knight RW, Stenchikov GL (1994) Changes of Snow Cover, Temperature, and Radiative Heat Balance over the Northern Hemisphere. J Clim 7:1633–1656. doi: 10.1175/1520-0442(1994)007

Hasegawa K, Matsuyama H, Tsuzuki H, Sweda T (2010) Improving the estimation of leaf area index by using remotely sensed NDVI with BRDF signatures. Remote Sens Environ 114:514–519. doi: 10.1016/j.rse.2009.10.005

Hope A, Engstrom R, Stow D (2005) Relationship between AVHRR surface temperature and NDVI in Arctic tundra ecosystems. Int J Remote Sens 26:1771–1776. doi: 10.1080/01431160500043780

Jia GJ, Epstein HE, Walker DA (2003) Greening of arctic Alaska, 1981–2001. Geophys Res Lett 30:2067. doi: 10.1029/2003GL018268

Laidler GJ, Treitz PM, Atkinson DM (2008) Remote Sensing of Arctic Vegetation: Relations between the NDVI, Spatial Resolution and Vegetation Cover on Boothia Peninsula, Nunavut. Arctic 61:1–13. doi: 10.2307/40513177

Landsat Science Team U (2010) Landsat Missions. In U.S.G.S. (USGS) (Ed.), Landsat.

Lillesand TM, Kiefer RW, Chipman JW (2007) Remote sensing and image interpretation. (sixth edition). Wiley

Lloyd AH, Yoshikawa K, Fastie CL, et al. (2003) Effects of permafrost degradation on woody vegetation at arctic treeline on the Seward Peninsula, Alaska. Permafr Periglac Process 14:93–101. doi: 10.1002/ppp.446

Lu D, Mausel P, Brondízio E, Moran E (2004) Change detection techniques. Int J Remote Sens 25:2365–2401. doi: 10.1080/0143116031000139863

Lundberg A, Beringer J (2005) Albedo and snowmelt rates across a tundra-to-forest transition. 15th Int. North. Res. Basins Symp. Workshop Luleaa Kvikkjokk Swed. 29 August - 2 Sept

Mack MC, Bret-Harte MS, Hollingsworth TN, et al. (2011) Carbon loss from an unprecedented Arctic tundra wildfire. Nature 475:489–492. doi: 10.1038/nature10283

Macleod RD, Congalton RG (1998) A quantitative comparision of change-detection algorithms for monitoring eelgrass from remotely sensed data. Photogramm Eng Remote Sens 64:207–216.

Maxwell SK, Sylvester KM (2012) Identification of “ever-cropped” land (1984-2010) using Landsat annual maximum NDVI image composites: Southwestern Kansas case study. Remote Sens Environ 121:186–195. doi: 10.1016/j.rse.2012.01.022

McDermid GJ, Franklin SE, LeDrew EF (2005) Remote Sensing for Large-Area habitat Mapping. Progress in Physical Geography 29:449–474

Oberbauer SF, Tweedie CE, Welker JM, et al. (2007) Tundra CO_2 fluxes in response to experimental warming across latitudinal and moisture gradients. Ecol Monogr 77:221–238.

Raynolds MK, Comiso JC, Walker DA, Verbyla D (2008) Relationship between satellite-derived land surface temperatures, arctic vegetation types, and NDVI. Remote Sens Environ 112:1884–1894. doi: 10.1016/j.rse.2007.09.008

Raynolds MK, Walker DA, Verbyla D, Munger CA (2013) Patterns of Change within a Tundra Landscape: 22-year Landsat NDVI Trends in an Area of the Northern Foothills of the Brooks Range, Alaska. Arct Antarct Alp Res 45:249–260.

Serreze MC, Walsh JE, Iii FSC, et al. (2000) Observational Evidence of Recent Change in the Northern High-Latitude Environment. Clim Change 46:159–207. doi: 10.1023/A:1005504031923

Silapaswan CS, Verbyla DL, McGuire AD (2001) Land Cover Change on the Seward Peninsula: The Use of Remote Sensing to Evaluate the Potential Influences of Climate Warming on Historical Vegetation Dynamics. 542–554.

Simms ÉL, Ward H (2013) Multisensor NDVI-Based Monitoring of the Tundra-Taiga Interface (Mealy Mountains, Labrador, Canada). Remote Sens 5:1066–1090. doi: 10.3390/rs5031066

Singh A (1989) Review Article Digital change detection techniques using remotely-sensed data. Int J Remote Sens 10:989–1003. doi: 10.1080/01431168908903939

Stone RS, Dutton EG, Harris JM, Longenecker D (2002) Earlier spring snowmelt in northern Alaska as an indicator of climate change. J Geophys Res. doi: 10.1029/2000JD000286

Stow DA, Hope A, McGuire D, et al. (2004) Remote sensing of vegetation and land-cover change in Arctic Tundra Ecosystems. Remote Sens Environ 89:281–308. doi: 10.1016/j.rse.2003.10.018

Tucker CJ (1979) Red and photographic infrared linear combinations for monitoring vegetation. Remote Sens Environ 8:127–150. doi: 10.1016/0034-4257(79)90013-0

USGS. Landsat 8 products: Background. Website. http://landsat.usgs.gov/landsat8.php Accessed 10 April 2014

Walker DA, Epstein HE, Raynolds MK, et al. (2012) Environment, vegetation and greenness (NDVI) along the North America and Eurasia Arctic transects. Environ Res Lett 7:015504. doi: 10.1088/1748-9326/7/1/015504

Walker DA, Jia GJ, Epstein HE, et al. (2003) Vegetation-soil-thaw-depth relationships along a low-arctic bioclimate gradient, Alaska: synthesis of information from the ATLAS studies. Permafr Periglac Process 14:103–123.

Williams M, Eugster W, Rastetter EB, et al. (2000) The controls on net ecosystem productivity along an Arctic transect: a model comparison with flux measurements. Glob Change Biol 6:116–126. doi: 10.1046/j.1365-2486.2000.06016.x

Xie Y, Sha Z, Yu M (2008) Remote sensing imagery in vegetation mapping: a review. J Plant Ecol 1:9–23. doi: 10.1093/jpe/rtm005